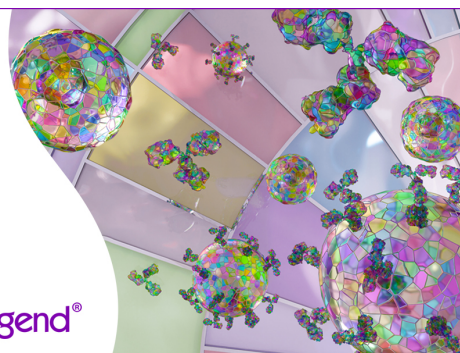


Discover 25+ Color Optimized Flow Cytometry Panels

- Human General Phenotyping Panel
- Human T Cell Differentiation and Exhaustion Panel
- Human T Cell Differentiation and CCRs Panel

Learn more ►

BioLegend®



The Journal of Immunology

RESEARCH ARTICLE | MARCH 06 2023

Prime-Pull Immunization of Mice with a BcfA-Adjuvanted Vaccine Elicits Sustained Mucosal Immunity That Prevents SARS-CoV-2 Infection and Pathology ✓

Mohamed M. Shamseldin; ... et. al

J Immunol (2023) 210 (9): 1257–1271.

<https://doi.org/10.4049/jimmunol.2200297>

Related Content

Intranasal immunization with an acellular pertussis vaccine containing a Th1/17 skewing adjuvant, BcfA, improves *B. pertussis* clearance from the mouse respiratory tract.

J Immunol (May,2018)

Cutting Edge: The Use of Topical Aminoglycosides as an Effective Pull in “Prime and Pull” Vaccine Strategy

J Immunol (April,2020)

Prime-Pull Immunization of Mice with a BcfA-Adjuvanted Vaccine Elicits Sustained Mucosal Immunity That Prevents SARS-CoV-2 Infection and Pathology

Mohamed M. Shamseldin,^{*,†,‡} Adam Kenney,^{*,1} Ashley Zani,^{*,1} John P. Evans,^{§,¶,1} Cong Zeng,^{§,¶,1} Kaitlin A. Read,^{*,1} Jesse M. Hall,^{*} Supanee Chaiwatpongsakorn,^{||} Mahesh K.C.,^{||} Mijia Lu,[§] Mostafa Eltohy,^{*} Parker Denz,^{*} Rajendar Deora,^{*,†} Jianrong Li,[§] Mark E. Peeples,^{||,§} Kenneth J. Oestreich,^{*} Shan-Lu Liu,^{*,†,§,¶} Kara N. Corps,[§] and Jacob S. Yount,^{*} and Purnima Dubey^{*}

Vaccines against SARS-CoV-2 that induce mucosal immunity capable of preventing infection and disease remain urgently needed. In this study, we demonstrate the efficacy of *Bordetella* colonization factor A (BcfA), a novel bacteria-derived protein adjuvant, in SARS-CoV-2 spike-based prime-pull immunizations. We show that i.m. priming of mice with an aluminum hydroxide- and BcfA-adjuvanted spike subunit vaccine, followed by a BcfA-adjuvanted mucosal booster, generated Th17-polarized CD4⁺ tissue-resident memory T cells and neutralizing Abs. Immunization with this heterologous vaccine prevented weight loss following challenge with mouse-adapted SARS-CoV-2 (MA10) and reduced viral replication in the respiratory tract. Histopathology showed a strong leukocyte and polymorphonuclear cell infiltrate without epithelial damage in mice immunized with BcfA-containing vaccines. Importantly, neutralizing Abs and tissue-resident memory T cells were maintained until 3 mo postbooster. Viral load in the nose of mice challenged with the MA10 virus at this time point was significantly reduced compared with naive challenged mice and mice immunized with an aluminum hydroxide-adjuvanted vaccine. We show that vaccines adjuvanted with alum and BcfA, delivered through a heterologous prime-pull regimen, provide sustained protection against SARS-CoV-2 infection. *The Journal of Immunology*, 2023, 210: 1257–1271.

Coronavirus disease of 2019 is a respiratory and multiorgan disease caused by SARS-CoV-2, a positive-sense RNA virus belonging to the family Coronaviridae, and the etiologic agent of the ongoing pandemic (1–3). To date, >660 million cases of infection and nearly 7 million deaths have been reported globally, making COVID-19 the worst pandemic since the 1918 influenza. Thus, there is a critical need to create a vaccine that will protect against primary infection and reinfection with the virus (4).

The symptoms of SARS-CoV-2 infection include headache, fever, chills, and a persistent dry cough. Additional symptoms may include gastrointestinal distress, diarrhea, vomiting, and loss of smell or taste.

The main transmission route of SARS-CoV-2 is via respiratory exposure, although infection may also occur via fecal–oral and ocular exposure (5). The causes of morbidity and mortality include pneumonia and the damaging cytokine storm elicited by infection, as well as multiorgan viral dissemination and organ failure in severe cases (6). Close person-to-person contact via virus-containing droplets and aerosols is the primary mode of SARS-CoV-2 transmission. Importantly, because asymptomatic individuals also transmit the infection (7, 8), there remains a need for vaccines that eliminate the viral load in the respiratory tract and prevent the development of a reservoir of asymptomatic individuals who serve as a silent source for transmission.

^{*}Department of Microbial Infection and Immunity, The Ohio State University, Columbus, OH; [†]Department of Microbiology, The Ohio State University, Columbus, OH; [‡]Department of Microbiology and Immunology, Faculty of Pharmacy, Helwan University–Ain Helwan, Helwan, Egypt; [§]Department of Veterinary Biosciences, The Ohio State University, Columbus, OH; [¶]Center for Retrovirus Research, The Ohio State University, Columbus, OH; ^{||}Center for Vaccines and Immunity, Abigail Wexner Research Institute at Nationwide Children's Hospital, Columbus, OH; and ^{||}Department of Pediatrics, The Ohio State University, Columbus, OH

¹A.K., A.Z., J.P.E., C.Z., and K.A.R. contributed equally to this work.

ORCIDs: 0000-0002-5324-1145 (M.M.S.); 0000-0001-8644-5825 (J.P.E.); 0000-0001-5704-5064 (K.A.R.); 0000-0003-3511-7359 (S.C.); 0000-0002-5177-9566 (M.K.C.); 0000-0002-4438-980X (M.L.); 0000-0002-4056-7429 (M.E.); 0000-0001-9420-1337 (P. Denz); 0000-0002-6093-8354 (R.D.); 0000-0002-4582-317X (M.E.P.); 0000-0002-3004-072X (K.J.O.); 0000-0003-1620-3817 (S.-L.L.); 0000-0002-5454-8421 (P. Dubey).

Received for publication April 20, 2022. Accepted for publication February 15, 2023.

This work was supported by The Ohio State University COVID-19 Seed Fund and National Institute of Allergy and Infectious Diseases Grants R21AI151867 (to P. Dubey) and R01AI125560 (to P. Dubey and R.D.), private donor funds (S.-L.L.), National Institute of Allergy and Infectious Diseases Grant R01AI090060 and National Institutes of Health Grant RM1HG008935 COVID-19 supplement award (to J.L.), National Institute of Allergy and Infectious Diseases Grant R01AI130110, National Heart, Lung, and Blood Institute Grant R01HL154001, National Cancer Institute Grant R01CA260582, and an American Lung Association COVID-19 and Emerging Respiratory Viruses Research Award (to J.S.Y.), National Institute of Allergy and Infectious Diseases Grant U19AI131386-04S1 (to M.E.P.), Nationwide Children's Hospital COVID-19 Seed Fund (to M.E.P.), National

Institute of Allergy and Infectious Diseases Grant R01AI134972 (to K.J.O.), and by National Institute of General Medical Sciences Grant T32GM068412. The Comparative Pathology & Digital Imaging Shared Resource and K.N.C. are supported in part by National Cancer Institute Grant P30CA16058MS. M.M.S. is supported by a doctoral fellowship from the Egyptian Bureau of Higher Education. A.Z. was supported by a National Science Foundation Graduate Fellowship. K.A.R. is supported by The Ohio State University College of Medicine Advancing Research in Infection and Immunity Fellowship Program.

M.M.S., J.M.H., and K.A.R. conducted immunological analysis; M.M.S., A.K., A.Z., M.E., and P. Denz conducted SARS-CoV-2 challenge, euthanasia, and TCID₅₀ assays; J.P.E. and C.Z. conducted virus neutralization assays; M.K.C. and M.L. purified MA10 virus; S.C. produced S protein; K.N.C. conducted histopathological analysis; P. Dubey designed the studies, and P. Dubey and M.M.S. analyzed data and wrote the manuscript; J.S.Y. supervised BSL-3 work; J.L. and M.E.P. supervised production of MA10 virus; M.E.P. supervised production of S protein; S.-L.L. supervised virus neutralization assays; K.J.O. supervised Tfh and GC B cell analysis; and R.D. and P. Dubey provided BcfA.

Address correspondence and reprint requests to Dr. Purnima Dubey, The Ohio State University, 460 West 12th Avenue, Biomedical Research Tower Rm. 784, Columbus, OH 43210. E-mail address: purnima.dubey@osumc.edu

The online version of this article contains supplemental material.

Abbreviations used in this article: A₄₅₀, absorbance at 450 nm; alum, aluminum hydroxide; BcfA, *Bordetella* colonization factor A; BSL-3, biosafety level 3; GC, germinal center; IHC, immunohistochemistry; i.n., intranasal; KO, knockout; N, nucleocapsid; PBST, PBS with Tween 20; PMN, polymorphonuclear cell; RT, room temperature; S, spike; T_{RM}, tissue-resident memory T cell; VAERD, vaccine-associated enhanced respiratory disease.

Copyright © 2023 by The American Association of Immunologists, Inc. 0022-1767/23/\$37.50

Emergency use authorization and subsequent U.S. Food and Drug Administration approval of mRNA vaccines, delivered i.m., altered the pandemic landscape, providing protection against severe disease and reducing mortality (9). These vaccines generate strong systemic neutralizing Ab responses that limit viral infection. Some studies have detected mucosal IgA and IgG following immunization of non-human primates and humans with mRNA vaccines (10–12). However, it is unclear whether these vaccines elicit tissue-resident memory T cell (T_{RM}) responses that are critical for preventing transmission and providing sustained protection against disease. Another important consideration in vaccine design is the possibility of vaccine-associated enhanced respiratory disease (VAERD), which is the development of a more severe form of disease manifested after vaccination against the causative agent (13–17). VAERD, which correlates with the Th2 immune responses, is elicited by whole cell-inactivated vaccines or Th2-skewing adjuvants such as aluminum hydroxide (alum). VAERD is reported as a side effect for inactivated vaccines against multiple pathogens, including respiratory syncytial virus (18, 19), measles (20, 21), and SARS-CoV and Middle East respiratory syndrome coronavirus, which are closely related to SARS-CoV-2 (22–25). Thus, novel vaccines and immunization regimens must be tested to ensure that they generate systemic and tissue-resident immune responses while limiting respiratory pathology.

In this study, we tested a subunit vaccine containing the soluble stabilized prefusion spike (S) protein of SARS-CoV-2 adjuvanted with the Th2-polarizing adjuvant alum alone or combined with the Th1/17-polarizing adjuvant Bordetella colonization factor A (BcfA) (26). BcfA is an outer-membrane protein of the animal pathogen *Bordetella bronchiseptica* (27) that has adjuvant function, eliciting systemic Ab and T cell responses to a variety of protein Ags (26). Notably, when combined with alum, BcfA attenuates Th2 responses primed by alum, thereby polarizing immune responses to Th1/Th17 (26).

To avoid enhanced respiratory disease (18, 28–32) we leveraged the ability of alum to induce a strong and safe systemic immune response with the ability of BcfA to attenuate alum-activated Th2-polarized immunity. To generate both systemic and mucosal immunity, we employed a prime-pull immunization regimen in mice with i.m. priming followed by an intranasal (i.n.) boost (33, 34). This regimen generated S-specific IgG and IgA in the serum and respiratory tract, with a higher ratio of mucosal IgG2/IgG1 compared with the alum-adjuvanted vaccine, as we previously observed with BcfA-adjuvanted *Bordetella* vaccines (26). Vaccines containing BcfA induced Th17-polarized $CD4^+ T_{RMS}$ whereas alum-adjuvanted vaccines generated Th2-polarized systemic and mucosal $CD4^+$ T cell responses. Mice immunized with either vaccine formulation were protected against both weight loss and viral replication in the upper and lower respiratory tract when challenged with mouse-adapted SARS-CoV-2. Importantly, the BcfA-adjuvanted vaccine efficiently protected the respiratory tract against infection-associated lung damage, whereas the vaccine adjuvanted with alum alone did not. T_{RMS} and neutralizing Abs were maintained until 3 mo postboost and reduced viral load in the nose of mice immunized with the BcfA-adjuvanted vaccine. Thus, the Th17-polarized mucosal and systemic T cell response, along with strong neutralizing Abs generated by systemic priming with an alum-BcfA-adjuvanted vaccine and mucosal booster with a BcfA-adjuvanted vaccine, prevented SARS-CoV-2-induced severe illness, virus replication, and respiratory pathology.

Materials and Methods

Biosafety

All experiments were performed in accordance with standard operating procedures at biosafety level 2 or biosafety level 3 (BSL-3) as appropriate. Work with live SARS-CoV-2 was performed in BSL-3 facilities according

to standard operating procedures approved by the Ohio State University BSL-3 Operations Group and Institutional Biosafety Committee. Samples were removed from the BSL-3 facility for immunohistochemistry (IHC) analysis or flow cytometry after fixation and decontamination using in-house validated and approved methods of sample decontamination.

Mice

All experiments were reviewed and approved by The Ohio State University Institutional Animal Care and Use Committee (protocol nos. 2020A00000054 and 2020A00000001). C57BL/6J mice and IL-17 knockout (KO) mice (male and female, >6 wk old) were bred in-house. Immunized and control naive mice were 16–20 wk old at the time of virus challenge.

Reagents

BcfA was produced and purified as described previously (26) with stringent endotoxin removal. The endotoxin level was <5 endotoxin units/mg protein. Stabilized S protein containing six proline substitutions was produced and purified as described (35). FBS and alum were from Sigma-Aldrich (St. Louis, MO). ELISA kits were from eBioscience (Thermo Fisher Scientific). Flow cytometry Abs were from eBioscience, BD Biosciences, or R&D Systems.

Isolation of mouse-adapted SARS-CoV-2 with an intact furin cleavage site

Mouse-adapted SARS-CoV-2 (strain MA10 generated by the laboratory of Dr. Ralph Baric, University of North Carolina) was obtained from BEI Resources (36). The provided stock was found to contain a mixture of wild-type (intact furin cleavage site within the virus S protein) and a large proportion of viruses with mutations/deletions in the furin cleavage site. To isolate a pure stock of SARS-CoV-2 MA10 containing the intact furin cleavage site, the virus was passaged once in primary, well-differentiated human bronchial epithelial cells to enrich for viruses that could infect these primary cells. Progeny virus was harvested at day 5 postinfection, serially diluted 10-fold, and used to inoculate Vero-TMPRSS2 cells in a plaque assay. At 2 d postinoculation, 50 individual small plaques were picked and used to inoculate one well of Vero-TMPRSS2 cells in a 12-well plate. The progeny virus from each well was harvested at day 2 postinoculation, and viral RNA was extracted from the harvested supernatant for RT-PCR with primers that amplify the region of the S gene encoding the furin cleavage site (forward, 5'-AAATCTATCAGGCCGGTAGC-3'; reverse, 5'-GAAGCCAGC ATCTGCAAGTG-3'). The PCR products were Sanger sequenced commercially using the forward primer. Four of 50 plaques were found to contain SARS-CoV-2 MA10 with the intact furin cleavage site. These viruses were grown in Vero-TMPRSS2 cells for another passage and sequenced again to confirm the presence of the intact furin cleavage site before being used in experiments.

Immunizations

Mice were lightly anesthetized with 2.5% isoflurane/O₂ for immunization. The i.m. immunization on day 0 was delivered in a 100- μ l vol divided between both forelimbs. The i.n. booster was inoculated in 50 μ l divided between both nares on days 28–35. Acellular vaccines contained 1 μ g of stabilized S alone (S) or mixed with 10 μ g of BcfA (S/B). S protein was adsorbed to 130 μ g of alum by rotating the suspension for 30 min at room temperature (S/A). Beads were pelleted and resuspended in 100 μ l of fresh PBS for i.m. injection or 50 μ l for i.n. instillation. S/A/B included 10 μ g of BcfA and 1 μ g of S adsorbed to alum as above.

Intravascular staining for discrimination between circulating and resident cells

Anti-CD45-PE (clone 30-F11, BD Biosciences) (3 μ g in 100 μ l of sterile PBS) was injected i.v. 10 min prior to sacrifice to label circulating lymphocytes, while resident lymphocytes are protected from labeling (37, 38). Peripheral blood was collected at the time of sacrifice and checked by flow cytometry to confirm that >90% of circulating lymphocytes were CD45-PE⁺.

Tissue dissociation and flow cytometry

Lungs were isolated and processed into a single-cell suspension using the gentleMACS tissue dissociator and the mouse lung dissociation kit (Miltenyi Biotec, catalog no. 130-095-927) followed by filtration through a 40- μ m filter and RBC lysis with ACK (ammonium-chloride-potassium) lysis buffer. Cells from each mouse were resuspended in T cell media (RPMI 1640 supplemented with 0.1% gentamicin, 10% heat-inactivated FBS, GlutaMAX, and 5×10^{-5} M 2-ME) and stimulated with PMA (50 ng/ml)/ionomycin (500 ng/ml) or with two pools of S peptides covering the C- and N- terminal (PepTivator SARS-CoV-2 Prot_S1 and PepTivator SARS-CoV-2 Prot_S+; (Miltenyi Biotec, catalog nos. 130-126-701 and 130-126-700) for 5–6 h at 37°C in the presence of protein transport inhibitor mixture (eBioscience). Peptide pools

were used at a final concentration of 1 $\mu\text{g}/\text{ml}$. A negative control group containing DMSO alone was included.

Following stimulation, cells were washed with cold PBS prior to staining with Live/Dead Zombie NIR fixable viability dye (BioLegend, catalog no. 423105) for 30 min at 4°C. Cells were then washed twice with PBS supplemented with 1% heat-inactivated FBS (1% FBS) (FACS buffer) and resuspended in Fc Block (clone 93) (eBioscience, catalog no. 14-0161-86) at 4°C for 5 min before surface staining with a mixture of the following Abs for 20 min at 4°C: CD3 V450 (clone 17A2; BD Biosciences, catalog no. 561389), CD4 BV750 (clone H129.19; BD Biosciences, catalog no. 747275), CD44 PerCP-Cy5.5 (clone IM7; BD Biosciences, catalog no. 560570), CD62L BV605 (clone MEL-14; BD Biosciences, catalog no. 563252), CD69 BV711 (clone HL2F3; BD Biosciences, catalog no. 740664), CD103 PE-CF594 (clone M290; BD Biosciences, catalog no. 565849). After two washes in FACS buffer, cells were resuspended in intracellular fixation buffer (eBioscience, catalog no. 00-8222-49) and incubated for 20 min at room temperature (RT). Following permeabilization (eBioscience, catalog no. 00-8333-56), intracellular staining (30 min at 4°C) was done using a mixture of the following Abs: IFN- γ FITC (clone XMG1.2; eBioscience, catalog no. 11-7311-82), IL-17 PE-Cy7 (clone eBio17B7; eBioscience, catalog no. 25-7177-82), and IL-5 allophycocyanin (clone TRFK5; BD Biosciences, catalog no. 554396). To identify CD8⁺ T cells, the same panel was used with CD8 allophycocyanin (clone 53-6.7; BioLegend, catalog no. 100712) and IFN- γ FITC only. Fluorescence minus one or isotype control Abs were used as negative controls. Finally, cells were washed with permeabilization buffer and resuspended in FACS buffer (PBS + 1% FBS). Samples were collected on a Cytex Aurora flow cytometer (Cytex Biosciences). Analysis was performed using FlowJo software version 10.8.0 according to the gating strategy outlined in Supplemental Figs. 1 and 2. The number of cells within each population was calculated by multiplying the frequency of live singlets in the population of interest by the total number of cells in each sample.

For the analysis of Th and germinal center (GC) B cell populations, mediastinal lymph nodes were harvested, and single-cell suspensions were generated in processing media (IMDM + 4% FBS) by passing tissue through a 100- μm cell strainer. Cells were incubated in 0.84% NH_4Cl for 3 min to lyse RBCs. After washing with processing media, cells were resuspended in FACS buffer (PBS + 4% FBS) supplemented with Fc Block (clone 93; BioLegend, catalog no. 101320) and incubated at 4°C for 5 min before staining. For surface staining, cells were incubated for 30 min at 4°C with the following Abs, as indicated: Ghost viability dye (1:400; Tonbo Biosciences, catalog no. 13-0870-T100), CD4 AF488 (1:300; clone GK1.5; R&D Systems, catalog no. FAB554G), CD44 BV421 (1:300; clone IM7; BD Biosciences, catalog no. 563970), CD62L allophycocyanin-eFluor 780 (1:300; clone MEL-14; Thermo Fisher Scientific, catalog no. 47-0621-82), PD-1 PE-Cy7 (1:50; clone 29F.1A12; BioLegend, catalog no. 135216), Cxcr5 allophycocyanin (1:50; clone SPRCL5; Thermo Fisher Scientific, catalog no. 17-7185-82), CD19 allophycocyanin (1:200; clone GL7, BioLegend, catalog no. 144610), GL7 PerCP-Cy5.5 (1:200; clone 1D3, BioLegend, catalog no. 152410), and Fas BV421 (1:300; clone Jo2; BD Biosciences, catalog no. 562633). Cells were then washed twice with FACS buffer and fixed using the eBioscience Foxp3 transcription factor staining kit (Thermo Fisher Scientific, catalog no. 00-5523-00), according to the manufacturer's instructions. Following fixation, cells were washed once with eBioscience 1 \times permeabilization buffer and twice with FACS buffer before resuspension in FACS buffer for analysis. Samples were analyzed on a BD FACSCanto II, and full analysis was performed using FlowJo software version 10.8.0.

Splenocyte stimulation and cytokine ELISA assays

Following dissociation and RBC lysis using ACK buffer, a single-cell suspension was plated at 2.5×10^6 cells/well of complete T cell medium (RPMI 1640, 10% FBS, 10 $\mu\text{g}/\text{ml}$ gentamicin, 5×10^{-5} M 2-ME) and stimulated with 1 $\mu\text{g}/\text{ml}$ S protein or with medium alone as a negative control. The supernatant was collected on day 3 poststimulation. The production of IFN- γ (R&D Systems, catalog no. DY485-05), IL-5 (Invitrogen, catalog no. 88-7054-88), and IL-17 (Invitrogen, catalog no. 88-7371-88) was quantified by a sandwich ELISA according to the manufacturers' instructions. Plates were read at absorbance at 450 nm (A_{450}) on a SpectraMax i3x plate reader and concentration was calculated based on the standard curve.

ELISA for S-specific Igs

Coming Costar high-binding 96-well ELISA plates (catalog no. 9018) were coated with 1 $\mu\text{g}/\text{ml}$ S protein in 1 \times PBS at 4°C overnight. Plates were washed three times with PBS with Tween 20 (PBST), blocked for 2 h at RT with ELISA diluent (Invitrogen, catalog no. 00-4202-56), and then washed twice with PBST. Serial dilutions of serum (1:500, 1:2,500, and 1:12,500 for IgG and IgA) and lung supernatant (1:500, 1:2,500, and 1:12,500 for IgG, 1:50 and 1:250 for IgA) samples were added and incubated for 2 h at RT.

Plates were washed four times with PBST and incubated with secondary anti-mouse IgG HRP (Abcam, catalog no. ab6789) or anti-mouse IgA HRP Abs for 1 h at RT. Plates were developed for 5–15 min at RT using 100 μl of tetramethylbenzidine (Invitrogen, catalog no. 50-112-9758) and the reaction was stopped with H_2SO_4 . Plates were read at A_{450} on a SpectraMax i3x plate reader. To evaluate Ab avidity, sodium thiocyanate (0–3 M) was added for 20 min at 37°C, prior to blocking and addition of detection Ab (39). The IgG relative avidity index was calculated as $[(A_{450} \text{ at } 2 \text{ M}) / (A_{450} \text{ at } 0 \text{ M})] \times 100$, and IgA relative avidity index was calculated as $[(A_{450} \text{ at } 1 \text{ M}) / (A_{450} \text{ at } 0 \text{ M})] \times 100$.

To determine IgG isotypes of S-specific Abs, plates were coated, blocked, and incubated with serum samples (1:5000), or lung homogenates were isolated following enzymatic digestion (1:1000) as described above. Rat anti-mouse Abs specific for IgG subtypes (IgG1, IgG2b, IgG2c, and IgG3; Invitrogen, catalog nos. 88-50630-88 and 88-50670-22) were added (1:1000 dilution) and incubated for 1 h at RT. Plates were washed four times with PBST, incubated with secondary anti-rat IgG HRP (1:5000; Rockland, catalog no. 612-1302) for 1 h at RT, and then developed with tetramethylbenzidine as above.

SARS-CoV-2 S pseudotyped lentivirus neutralization assay

Virus neutralization by serum and lung Abs was performed as described (40). We used 100 μl of *Gussia* luciferase reporter gene-bearing lentivirus pseudotyped with the wild-type S or BA.4/BA.5 (Omicron) variant S protein in each well of a 96-well plate. Virus was incubated with 4-fold serial dilutions of serum/lung homogenates for 1 h at 37°C (final dilutions 1:40, 1:160, 1:640, 1:2,560, 1:10,240, and no serum control). Media (DMEM [Life Technologies, catalog no. 11965-092] supplemented with 10% [v/v] FBS [Life Technologies, catalog no. 11965-092] and 1% [v/v] penicillin/streptomycin [HyClone, catalog no. SV30010]) was removed from seeded HEK293T/ACE2 cells (BEI Resources, catalog no. NR-52511) and replaced with the virus/serum mixture. Cells were cultured for 6 h at 37°C before changing to fresh media. *Gussia* luciferase activity was measured at 24, 48, and 72 h after media change. For luciferase measurement, 20 μl of supernatant was collected from each well and transferred to a white nonsterile 96-well plate. To each well, 20 μl of *Gussia* luciferase substrate (0.1 M Tris [MilliporeSigma, catalog no. T6066] at pH 7.4, 0.3 M sodium ascorbate [Spectrum Chemical, catalog no. S1349], 10 μM coelenterazine [GoldBio, catalog no. CZ2.5]) was added, and luminescence was immediately read by a BioTek Cytation 5 plate reader. Fifty percent neutralization titers were determined by least-squares nonlinear regression in GraphPad Prism 5.

SARS-CoV-2 MA10 infection and viral titer measurements

Mice were anesthetized with inhaled isoflurane in oxygen and were i.n. infected with 5×10^4 PFU of SARS-CoV-2 MA10 diluted in PBS where indicated. Clinical signs of disease (weight loss) were monitored daily. Mice were euthanized by isoflurane overdose at 2 d postinfection, and samples for titer (caudal right lung lobe and nasal septum) and histopathological analyses (left lung lobe) were collected. Importantly, mice were randomized and assigned to specific harvest days before the start of the experiment. Lung and nose viral titers were determined by plaque assay. Briefly, right caudal lung lobes and nasal septum were homogenized in PBS using glass beads, and serial dilutions of the clarified lung homogenates were added to a monolayer of Vero E6 cells. After 3 d, the cytopathic effect was examined via staining for viral nucleoprotein (Sino Biological, catalog no. 40143-MM08-100). The left lung lobe was stored in 10% phosphate-buffered formalin for 7 d prior to removal from the BSL-3 for processing. After paraffin embedding, sectioning, and staining, histopathological scoring was performed.

Lung histopathology and immunohistochemistry

Lung samples from mice were processed per a standard protocol. Briefly, the tissues were fixed in 10% neutral-buffered formalin. Tissues were processed and embedded in paraffin. Five-micrometer sections (three per tissue) were stained with H&E by the Comparative Pathology & Mouse Phenotyping Shared Resource at The Ohio State University or at HistoWiz. A board-certified veterinary pathologist (K.N.C.) was blinded to the experimental groups, and sections were scored qualitatively on a scale ranging from 0 to 5 for the degree of cellularity and consolidation, the thickness of the alveolar walls, degeneration and necrosis, edema, hemorrhage, infiltrating alveolar/interstitial polymorphonuclear cells (PMNs), intrabronchial PMNs, perivascular and peribronchial lymphocytes and plasma cells, and alveolar macrophages. The total inflammation score was calculated by totaling the qualitative assessments in each category.

Immunohistochemistry to detect nucleocapsid (N) protein expression in lung sections was conducted by HistoWiz. Briefly, tissue sections were stained with a rabbit monoclonal anti-N Ab (GeneTex, catalog no. GTX635686) using standard methodology.

Statistical analysis

Serological responses, T and B cell readouts, mouse weights, and viral titer data were analyzed using GraphPad Prism 9.3 with the methods outlined in each figure legend.

Results

Intramuscular priming with S/A/B and intranasal booster with S/B elicits Th17-polarized mucosal and systemic T cell responses

We tested a subunit vaccine containing the soluble prefusion S protein (Washington strain) with six stabilizing proline substitutions (35) as the Ag, adjuvanted with alum alone, or alum and BcfA.

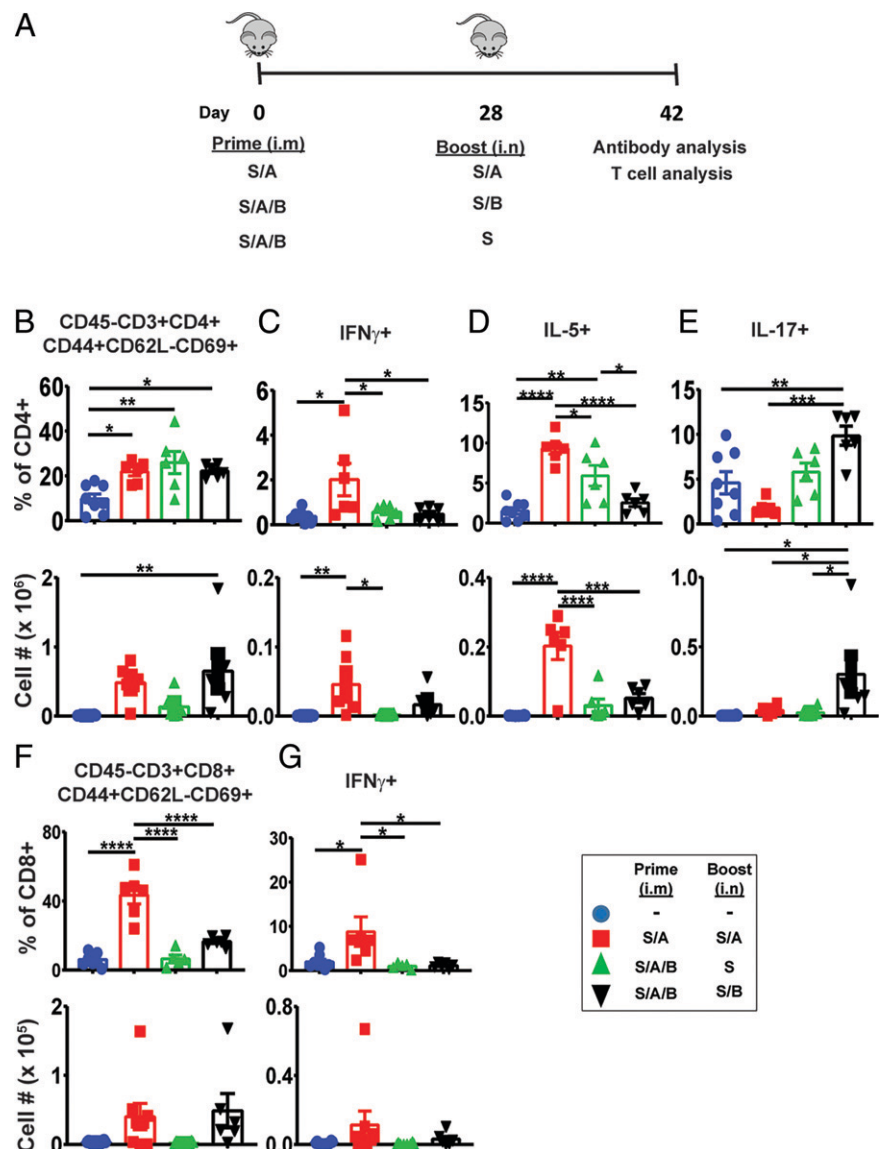
We immunized C57BL/6 mice i.m. with 1 μ g of S adsorbed to alum (S/A) or S protein with alum and 10 μ g of BcfA (S/A/B). We previously established that this adjuvant combination and dosage used in combination with Ags from the bacterial pathogen, *Bordetella pertussis*, elicit protective immunity in a murine model (26). On day 28, mice were boosted i.n. with S alone, S/A, or with S/B and evaluated at 14 d postboost (Fig. 1A). To distinguish between tissue-resident and circulating T cells in the lungs, we injected mice i.v. with anti-CD45-PE 10 min prior to euthanasia (37, 38). Lungs were enzymatically dissociated, single-cell suspensions were stimulated with PMA/ionomycin, and cells were stained with Abs against CD3,

CD4 or CD8, CD44, CD62L, and CD69. Cells were fixed, permeabilized, and stained with anti-IFN- γ , anti-IL-17, and anti-IL-5 Abs.

Compared to naive mice, the percentage of CD45⁺CD3⁺CD4⁺CD44⁺CD62L⁺CD69⁺ T_{RM}s increased in all vaccinated groups (Fig. 1B; see Supplemental Fig. 1 for the gating strategy), whereas the number of CD4⁺ T_{RM}s was only significantly increased in mice primed with S/A/B and boosted with S/B (Fig. 1B). Mice primed and boosted with S/A produced IFN- γ (Fig. 1C) and IL-5 (Fig. 1D), whereas mice primed with S/A/B and boosted with S/B produced primarily IL-17 (Fig. 1E). Notably, inclusion of BcfA in the vaccine significantly attenuated the proportion and number of IL-5-producing CD4⁺ T_{RM}s (Fig. 1D). The percentage of CD8⁺ T_{RM}s (Fig. 1F) that produced IFN- γ (Fig. 1G) increased in S/A-immunized mice, but not in mice primed with S/A/B and boosted with S/B, suggesting that BcfA primarily elicited CD4⁺ T cells.

To understand the systemic T cell response to vaccination, we next examined circulating (CD45⁺) memory T cells in lung single-cell suspensions. Mice immunized with either vaccine had a higher percentage of CD45⁺CD4⁺CD44⁺CD62L⁺CD69⁺ T cells in the lungs compared with naive mice whereas the number of these cells significantly increased in mice primed with S/A/B and boosted with S/B (Fig. 2A). The T cells of mice primed and boosted with S/A produced IFN- γ (Fig. 2B) and IL-5 (Fig. 2C), but negligible IL-17 (Fig. 2D),

FIGURE 1. BcfA mucosal booster elicits Th17-polarized resident CD4⁺ lung memory T cells and attenuates Th2 responses elicited by alum. (A) Prime-pull immunization strategy to elicit mucosal immune response in C57BL/6 mice. Mice (six per group) were 5injected i.m. on day 0 and inoculated i.n. on day 28 with various vaccine formulations, with analysis of T cell populations in the lungs conducted on day 42 (2 wk postboost). Mice were injected i.v. with CD45-PE Ab 10 min before euthanasia to distinguish between resident (CD45⁺) and circulating (CD45⁺) T cells. (B–E) Percentage and number of CD45⁺CD3⁺CD4⁺CD44⁺CD62L⁺CD69⁺ Ag-experienced CD4⁺ T_{RM}s (B) as well as the percentage and number of IFN- γ ⁺ (C), IL-5⁺ (D) and IL-17⁺ (E) cells are shown. Gating strategy is shown in Supplemental Fig. 1. (F and G) Percentage and number of CD45⁺CD3⁺CD8⁺CD44⁺CD62L⁺CD69⁺ Ag-experienced CD8⁺ T_{RM}s (F) and the IFN- γ ⁺ subset (G) are shown. One-way ANOVA with a Tukey's multiple comparisons test was used to detect differences between all experimental groups. Significance is indicated above for each group (* p < 0.05, ** p < 0.01, *** p < 0.001, **** p < 0.0001). The data are representative of two independent experiments. Mean and SEM are displayed.



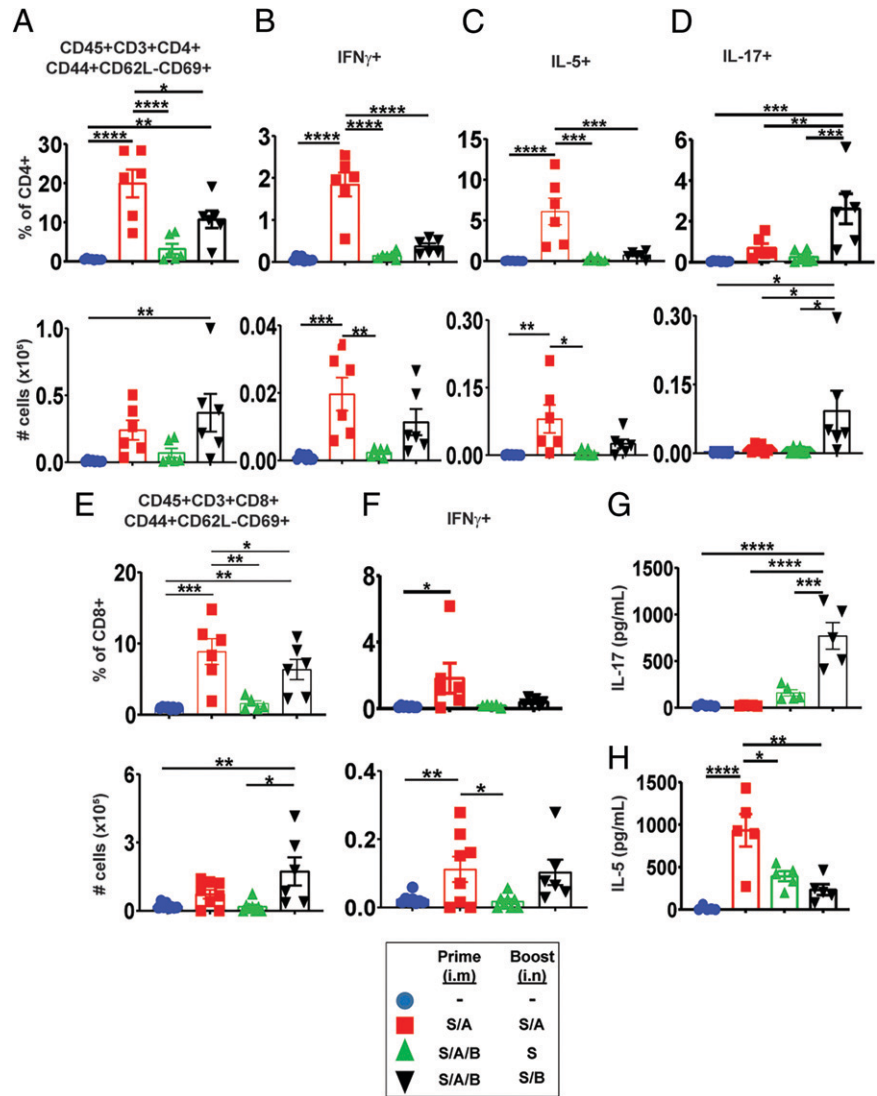


FIGURE 2. BcfA-adjuvanted vaccines elicit Th17-polarized systemic T cell immunity. Lung cells (from mice in Fig. 1; six per group) were analyzed for the presence of CD45⁺ circulating T cells. (A) Percentage and number of CD45⁺CD3⁺CD4⁺CD44⁺CD62L⁻CD69⁺ Ag-experienced CD4⁺ T_{RM}s are shown. (B–D) Percentage and number of IFN-γ⁺ (B), IL-5⁺ (C), and IL-17⁺ (D) cells are shown. (E) Percentage and number of CD45⁺CD3⁺CD8⁺CD44⁺CD62L⁻CD69⁺ Ag-experienced CD8⁺ T_{RM}s are shown. (F) Percentage and number of IFN-γ⁺ subset are shown. Splenocytes were isolated and processed into single-cell suspensions before stimulation with 1 μg of S protein. (G and H) IL-17 (G) and IL-5 (H) present in the culture supernatant at 3 d poststimulation were determined by ELISA. Differences between all experimental groups were analyzed by one-way ANOVA with a Tukey's multiple comparisons test. **p* < 0.05, ***p* < 0.01, ****p* < 0.001, *****p* < 0.0001. Mean and SEM are shown.

indicating generation of a Th1/2-polarized immune response. In mice primed with S/A/B and boosted with S/B, circulating memory CD4⁺ T cells did not produce IFN-γ (Fig. 2B) or IL-5 (Fig. 2C) and only produced IL-17 (Fig. 2D). Compared to naive mice, the percentage and number of CD45⁺CD8⁺CD44⁺CD62L⁻CD69⁺ T cells increased with either alum or alum and BcfA-containing vaccines (Fig. 2E). However, the proportion and number of IFN-γ-producing cells only increased in S/A-immunized mice (Fig. 2F).

We then tested the cytokines produced by spleen cells of immunized mice following stimulation with S protein for 72 h. Spleen cells of mice primed with S/A/B and boosted with S/B produced IL-17 (Fig. 2G) but negligible IL-5 (Fig. 2H). Spleen cells of S/A-primed and boosted mice primarily produced IL-5 (Fig. 2H) whereas IFN-γ was not detected in supernatants of any of the groups (data not shown). Thus, S/A/B prime and S/B boost elicited Th17-polarized systemic responses, overriding the Th2-skewed responses elicited by alum.

We then evaluated whether immunization with BcfA-containing vaccines generated Ag-specific T_{RM}s. Dissociated lung cells were stimulated with peptide pools derived from S and stained as described above. The percentage and number of Ag-experienced cells increased in mice primed with S/A/B and boosted with S/B (Fig. 3A). These cells did not produce significantly more IFN-γ (Fig. 3B) or IL-5 (Fig. 3C) than did naive mice or S/A-immunized mice and produced only IL-17 (Fig. 3D). The proportion and number of Ag-experienced and cytokine-producing cells did not increase in mice immunized with

S/A/B and boosted with S alone, compared with naive mice or mice that received the S/B booster. Thus, the inclusion of BcfA in the mucosal boost generated Ag-specific T_{RM}s in the lungs. Interestingly, although the proportion and number of Ag-specific circulating (CD45⁺) memory T cells increased (Fig. 3E), changes in the percentage and number of cytokine-producing cells did not reach statistical significance. This result suggests that the Ag-specific cells were largely tissue-resident. Furthermore, this vaccine did not elicit Ag-specific CD8⁺ T cells (data not shown).

Overall, the addition of BcfA to the priming immunization and a booster with BcfA as the sole adjuvant elicited Th17-polarized systemic and mucosal CD4⁺ T cells and significantly attenuated IL-5 responses primed by alum.

Prime-pull immunization generated Tfh and GC B cells in the draining lymph nodes

Tfh cells are a specialized Th cell subset that play a critical role in support of Ab production by B cells (41). We examined whether our prime-boost immunization regimen and vaccines generated Tfh cell populations. Indeed, we observed Tfh (PD-1^{hi}CXCR5^{hi}) cells in the draining mediastinal lymph nodes of mice immunized with S/A alone or primed with S/A/B and boosted with S/B (Fig. 4A). As Tfh populations support B cell activation and neutralizing Ab production, we also determined whether our immunization regimen and vaccines supported the activation of GC B cells (42, 43). All adjuvanted

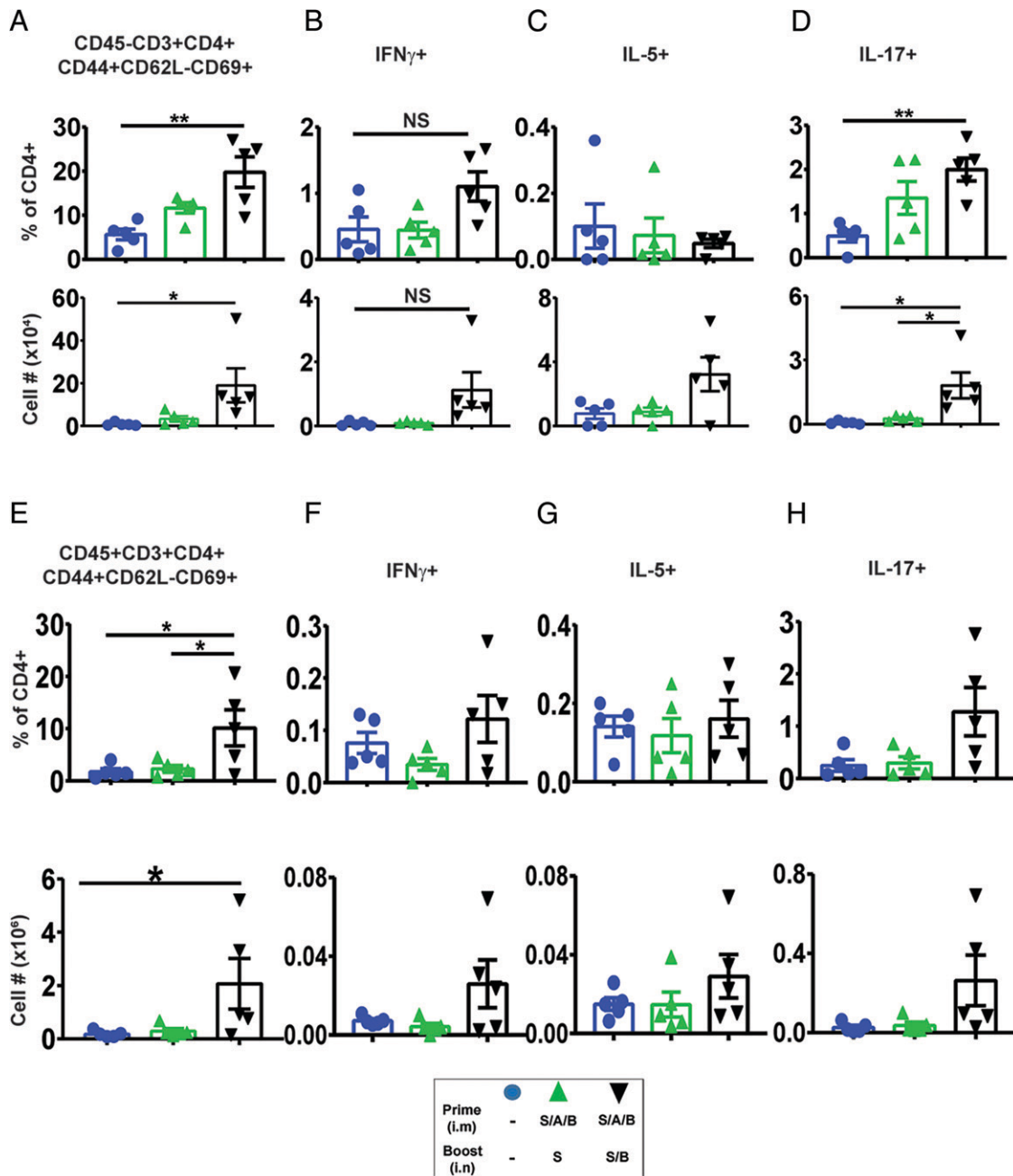


FIGURE 3. BcfA-adjuvanted mucosal booster elicits S-specific Th17-polarized lung-resident CD4⁺ T_{RM}S. Lung cells were stimulated for 6 h with S-derived peptide pools (S1 and S2) at a concentration of 1 μg/ml in the presence of protein transport inhibitors. Surface staining and ICS were conducted to analyze both CD45⁺ resident and CD45⁺ circulating T cells. **(A)** Percentage and number of CD45⁺CD3⁺CD4⁺CD44⁺CD62L⁺CD69⁺ Ag-experienced CD4⁺ T_{RM}S are shown. **(B–D)** Percentage and number of IFN-γ⁺ (B), IL-5⁺ (C), and IL-17⁺ (D) cells are shown. **(E)** Percentage and number of CD45⁺CD3⁺CD4⁺CD44⁺CD62L⁺CD69⁺ Ag-experienced CD4⁺ T_{RM}S are shown. **(F–H)** Percentage and number of IFN-γ⁺ (F), IL-5⁺ (G), and IL-17⁺ (H) subsets are shown. One-way ANOVA with a Tukey's multiple comparisons test was used to detect differences between all experimental groups. **p* < 0.05, ***p* < 0.01. *n* = 5 animals per group; mean and SEM of the results are displayed.

vaccines generated activated (Fas⁺GL7⁺) GC B cells (Fig. 4B) compared with naive mice. Supplemental Fig. 2 shows the gating strategy. Taken together, these data suggest that systemic priming with an alum-containing vaccine activates Tfh and GC B cell responses that promote S-specific Ab production.

BcfA-adjuvanted vaccines elicit Th1-polarized mucosal and systemic IgG Abs

Generation of S-specific Abs by vaccination is correlated with protection against SARS-CoV-2 (13, 16). We examined whether the prime-pull immunization regimen generated both mucosal and systemic

Abs. We quantified the S-specific IgG and IgA Abs in the lungs of naive and immunized mice. All immunized groups of mice had higher IgG Abs in the lungs compared with naive mice (Fig. 5A). S/A- and S/B-boosted mice had higher Abs than did mice boosted with S alone, suggesting that an adjuvant is important for generating mucosal Abs. Additionally, the avidity of S-specific IgG, determined by addition of sodium thiocyanate (39), was higher in the mice that received the S/B booster compared with booster with S alone (Fig. 5B). We then tested whether the addition of BcfA altered the Th1/Th2 polarization of the mucosal Abs. Mice boosted with S/B had a higher ratio of IgG2b/IgG1 compared with booster with S alone and

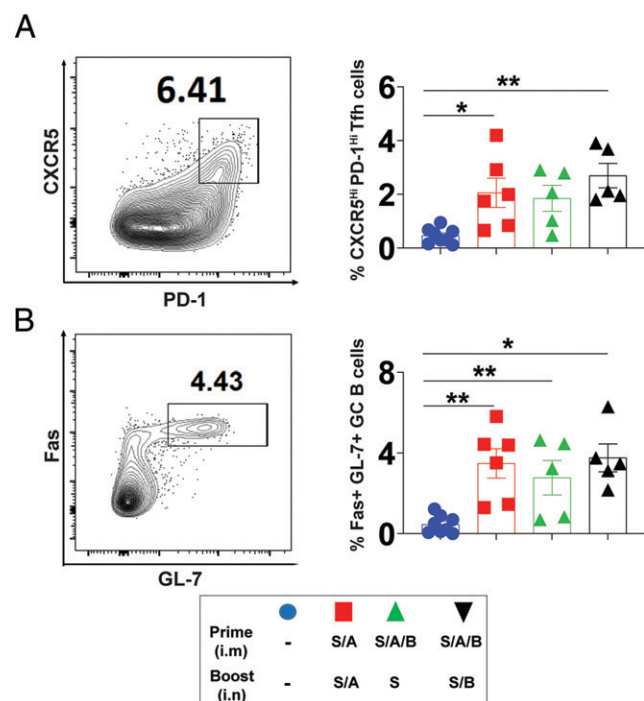


FIGURE 4. Immunization with alum- or alum+BcfA-adjuvanted vaccines generates PD-1^{high}CXCR5^{high} (Tfh) cells and Fas⁺GL7⁺ (GC B) cells in the draining mediastinal lymph node. Single-cell suspensions of the draining (mediastinal) lymph nodes were evaluated for presence of Tfh and GC B cell populations. Tfh populations were identified as activated (CD44⁺) PD-1^{hi} CXCR5^{hi} cells. GC B cell populations were identified as Fas⁺GL7⁺ cells. **(A)** Percentage of Tfh out of total CD4⁺ cells. **(B)** Percentage of GC B cells out of total CD19⁺ B cells. One-way ANOVA with a Tukey's multiple comparisons test was used to detect differences between all experimental groups. * $p < 0.05$, ** $p < 0.01$. $n = 6$ animals per group. Data are displayed as mean and SEM and are representative of two independent experiments.

higher IgG2c/IgG1 compared with mice primed and boosted with S/A or primed with S/A/B and boosted with S alone (Fig. 5C). Thus, the combination of alum and BcfA as adjuvants increased mucosal IgG Ab avidity and skewed the overall IgG response toward the Th1 phenotype.

We then quantified the relative amounts of S-specific IgG in the serum. All groups immunized with adjuvanted vaccines had specific serum Abs at levels higher than those of naive mice (Fig. 5D). The relative amount of Ab was higher in mice that received either S/A or S/B in the booster compared with S alone (Fig. 5D), suggesting that an adjuvant in the mucosal booster increased the amount of circulating IgG Abs and IgG Ab avidity (Fig. 5E). The serum IgG2/IgG1 ratio did not differ between S/A- or S/A/B-immunized groups (Fig. 5F).

Prime-pull immunization generated mucosal and systemic IgA

We found that immunization with S/A or S/A/B_S/B generated IgA in the lungs (Fig. 5G) and in the serum (Fig. 5H), demonstrating that the mucosal booster induces IgA locally and systemically. In contrast, as previously reported, systemic immunization with alum-adjuvanted S-containing vaccines does not generate circulating IgA responses (13). Thus, IgA elicited by a mucosal booster also enters the circulation.

Immunization of mice with S/A or S/A/B prevented SARS-CoV-2 infection associated weight loss and reduced viral titers in the respiratory tract

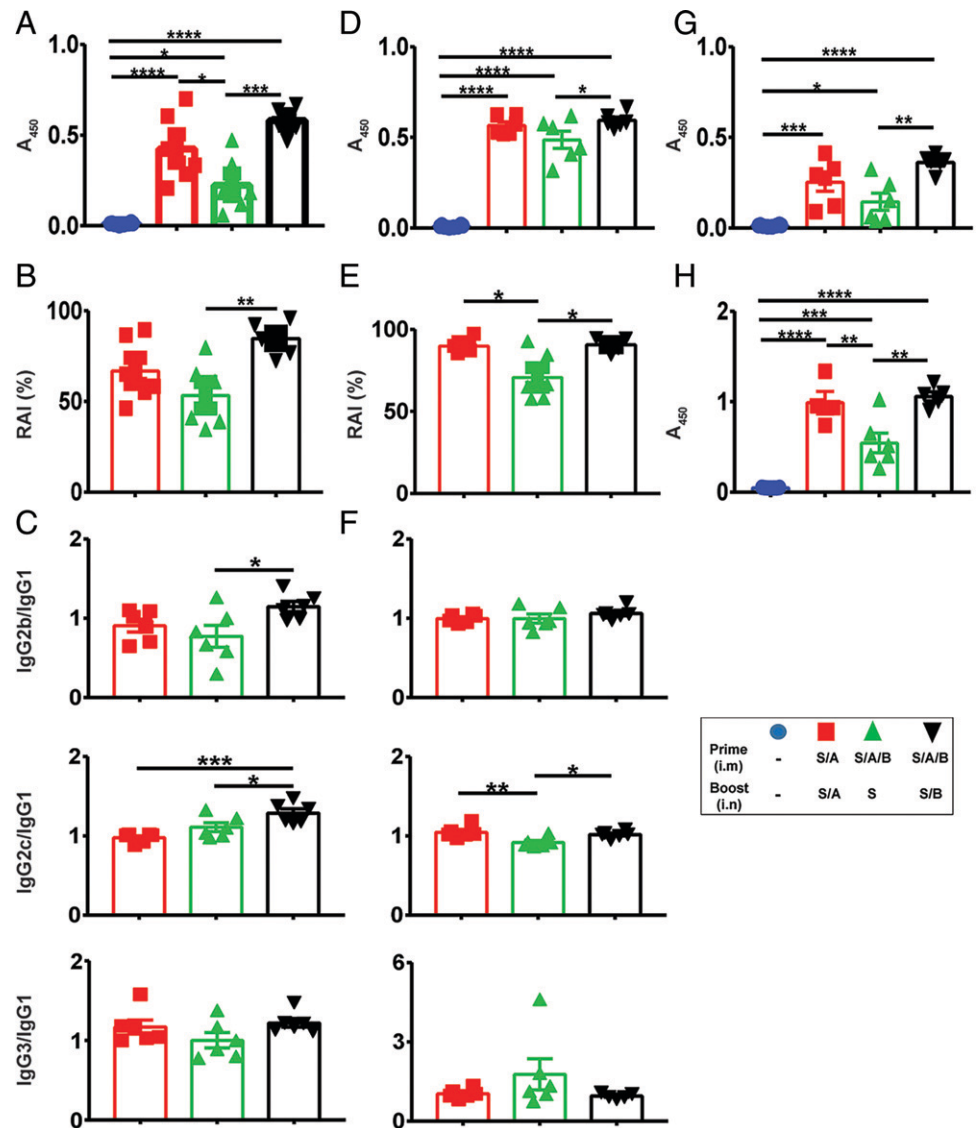
To determine whether our immunization regimens prevented virus infection in vivo, we challenged naive and immunized mice i.n. with 5×10^4 PFU of mouse-adapted SARS-CoV-2 (strain MA10)

(Fig. 6A). We recorded daily body weight in one cohort of infected mice until day 10 postinfection to assess whether immunization affected disease severity. Naive infected mice and mice immunized with S alone lost 10–15% body weight beginning on day 2 postinfection and recovered to prechallenge weight by day 8 postinfection (Fig. 6B). In contrast, mice immunized and boosted with S/A or immunized with S/A/B and boosted with S/B did not lose weight (Fig. 6B), indicating that the vaccines prevented severe disease. We quantified viral load in the nose and lungs on day 2 postinfection in a second cohort infected at the same time. In wild-type C57BL/6 mice viral load in the nose (Fig. 6C) and lungs (Fig. 6D) was 5–6 logs lower in both vaccinated groups compared with S-immunized or naive mice. Thus, a vaccine adjuvanted with alum alone, or alum and BcfA, prevented virus-associated weight loss and virus infection of the upper and lower respiratory tract. We then tested the contribution of IL-17 generated by the BcfA-containing vaccine to protection and reduction of respiratory viral burden. We immunized IL-17 KO mice i.m. with S/A/B and boosted i.n. with S/B on days 0 and 28, respectively. Naive and immunized IL-17 KO mice were challenged with MA10 virus 14 d later. S/A/B_S/B-immunized IL-17 KO mice did not lose weight (Fig. 6E), suggesting that protection against severe disease was unaffected by the lack of IL-17-producing cells. However, viral load in the nose (Fig. 6F) was similar in naive and immunized IL-17 KO mice and reduced by only ~1 log in the lungs (Fig. 6G). These data suggest that IL-17 produced by immunization with the BcfA-adjuvanted vaccine contributes to virus clearance. IgA, IgG, and IgG isotypes were unaffected in the lungs of immunized IL-17 KO mice (Supplemental Fig. 3), suggesting that the Ab response was not altered by the absence of IL-17. These data further imply that the inability of S/A/B_S/B-immunized IL-17 KO mice to reduce viral load in the respiratory tract is due to the absence of IL-17-producing cells.

Marked lymphocyte and PMN infiltrate without epithelial damage following SARS-CoV-2 challenge in the lungs of mice primed with S/A/B and boosted with S/B

We evaluated formalin-fixed, paraffin-embedded lung sections harvested on day 2 postinfection to determine the extent of pneumonia, immune cell infiltration, and epithelial damage. Histopathological evaluation of sections stained with H&E detected marked hemorrhage (filled arrows) and edema (open arrows) around blood vessels and airways in naive challenged mice (Fig. 7A) and mice immunized with S alone (Fig. 7B). Mixed eosinophilic proteinaceous debris was often admixed, sometimes near vessels rimmed by hemorrhage. Significant type II pneumocyte hyperplasia (asterisks) was evident in affected areas, resulting in moderate to marked thickening of alveolar walls, often accompanied by infiltration of large macrophages. Bronchioles exhibited degeneration and necrosis (ovals), with necrotic cellular debris, and blebbing apical epithelial cell debris. Mice primed and boosted with S/A displayed a focal pattern of hemorrhage and edema with milder degeneration and airway necrosis (Fig. 7C). Large foamy macrophage infiltration was observed with some lymphocyte aggregates (arrows) in perivascular spaces with little edema. Eosinophilic debris was less evident in this group. Mice primed with S/A/B and boosted with S/B (Fig. 7D) showed comparably mild thickening of alveolar walls, mild degeneration of bronchiolar epithelium, some perivascular and vascular inflammation, and a marked increase in perivascular and peribronchiolar lymphocytic aggregates with mitoses (tailed arrows), suggesting expansion of the lymphoid population. The absence of epithelial damage was notable in this group. Semiquantitative scoring showed reduced thickening of alveolar walls (Fig. 7E), reduced alveolar macrophages (Fig. 7F), and reduced degeneration and necrosis (Fig. 7G) in mice immunized with S/A/B_S/B compared with naive challenged mice. Lymphocytes

FIGURE 5. BcfA mucosal booster generates Th1-polarized mucosal and systemic Abs. ELISA analysis evaluated S-specific Abs in lung homogenates and serum. **(A)** S-specific IgG in lung homogenates at 1:1250 dilution. **(B)** Sodium thiocyanate (NaSCN) at 2 M was added to the ELISA to measure Ab avidity of S-specific IgG in lung homogenates. Relative avidity index (RAI) was calculated as follows: $[(A_{450} \text{ at } 2 \text{ M}) / (A_{450} \text{ at } 0 \text{ M})] \times 100$. **(C)** S-specific IgG isotypes in lung homogenates were determined using specific secondary Abs. The ratio of each IgG2 subclass to IgG1 is shown. **(D)** S-specific IgG in serum at 1:12,500 dilution. **(E)** RAI of serum IgG was calculated with the addition of 2 M sodium thiocyanate in the ELISA. **(F)** Ratio of each IgG2 subclass to IgG1 in serum. **(G)** IgA in lung homogenates at 1:50 dilution. **(H)** IgA in serum at 1:12500 dilution. Differences between experimental groups were determined by one-way ANOVA with a Tukey's multiple comparisons test. * $p < 0.05$, ** $p < 0.01$, *** $p < 0.001$, **** $p < 0.0001$. $n = 6$ animals per group. Data are representative of two independent experiments. Mean and SEM of the results are displayed.



were increased in this group compared with naive challenged mice (Fig. 7H). We then tested the presence of SARS-CoV-2 N protein as a second measure of virus presence in the lungs. IHC analysis revealed strong and widespread N protein staining in epithelial cells of naive challenged mice (Fig. 7I) and mice immunized with S alone (Fig. 7J). Mice primed and boosted with S/A showed foci of N protein staining in two of five mice (Fig. 7K, Supplemental Table I), suggesting that protection from infection was inefficient in this group. Remarkably, N protein staining was completely absent from the lungs of all mice immunized with S/A/B and boosted with S/B (Fig. 7L, Supplemental Table I), suggesting either that this vaccine combination prevented infection more efficiently, or that the more robust immune cell infiltrate accelerated clearance of virally infected cells and debris. Thus, histopathological and IHC analysis revealed that priming mice with S/A/B and boosting with S/B prevented viral infection and respiratory disease.

Histopathology of lungs from naive and immunized IL-17 KO mice showed milder pathology overall compared with wild-type mice. Naive challenged mice displayed thickening of the alveolar wall with hemorrhage, type II pneumocyte hyperplasia and inflammation, degeneration and sloughing in the airways with an inflammatory infiltrate, and tissue necrosis (Fig. 8A). Lungs of immunized IL-17 KO mice also displayed hemorrhage, necrosis, airway degeneration,

and type II pneumocyte hyperplasia. Lymphoid expansion, congestion, and hypercellularity were also observed (Fig. 8B). Histopathology quantification showed a slight increase in alveolar wall thickening (Fig. 8C) and no change in alveolar macrophages (Fig. 8D) or necrosis (Fig. 8E) in immunized mice. Infiltration of lymphocytes and plasma cells was significantly higher (Fig. 8F) in immunized mice compared with naive mice, suggesting that although the immunization recruited lymphocytes to the tissues, these did not have antiviral function. These data show that although IL-17 KO mice had milder respiratory disease compared with wild-type C57BL/6 mice, immunized mice were not protected from respiratory pathology. Thus, Th17-polarized T cells generated by BcfA-adjuvanted vaccines contribute to prevention of respiratory damage following SARS-CoV-2 challenge. IHC did not detect N protein staining in lungs of IL-17 KO naive or immunized mice (data not shown), likely due to the overall lower viral titer in the respiratory tract compared with wild-type C57BL/6 mice.

Nasal viral titer is reduced in S/A/B_S/B-immunized mice challenged at 3 mo postboost

We then tested whether these experimental vaccines provided sustained protection against infection. Naive mice and mice immunized with S/A_S/A or S/A/B_S/B were challenged with 5×10^4 PFU of MA10 virus at 3 mo postbooster immunization. One cohort of animals

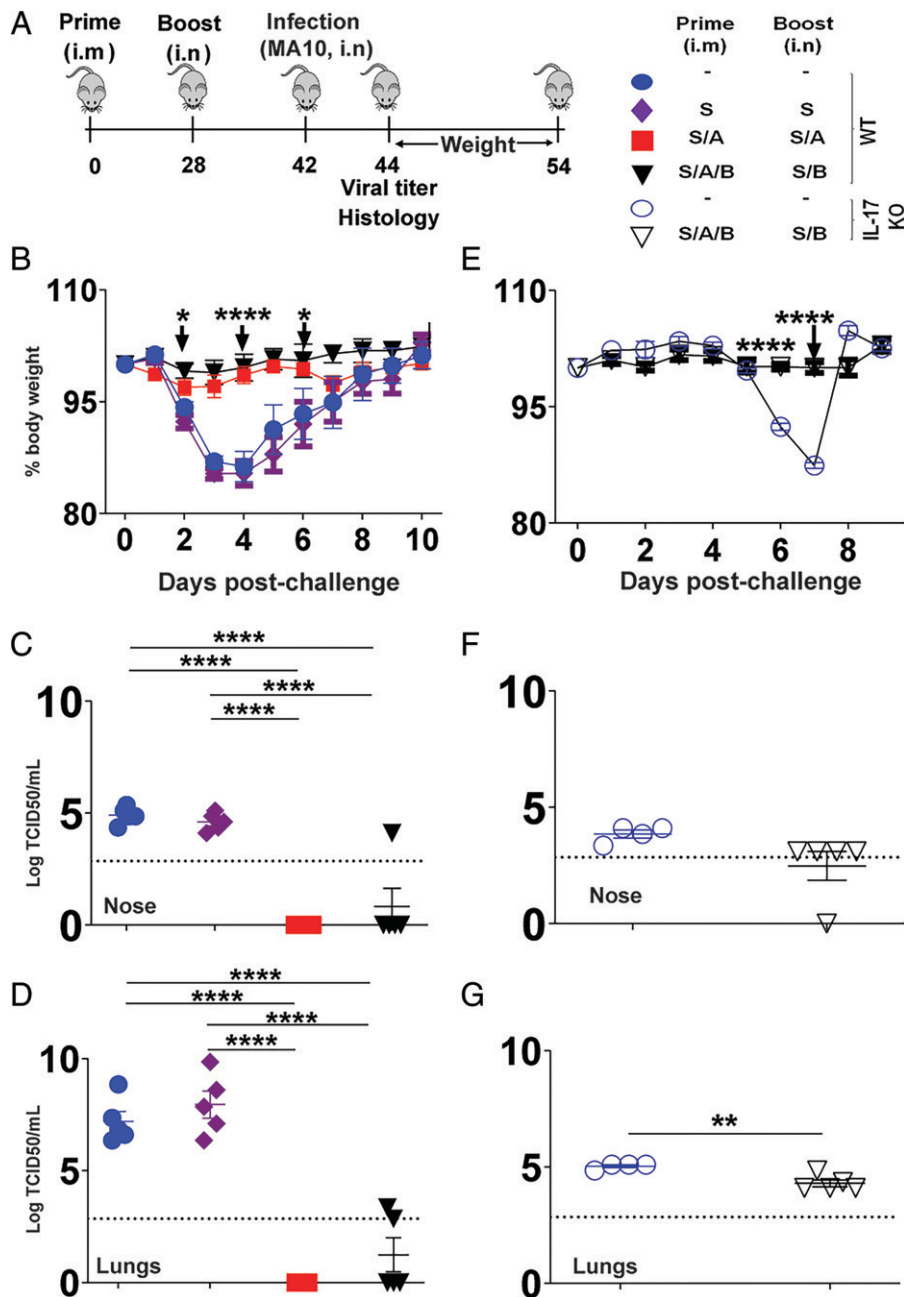


FIGURE 6. Prime-pull immunization with either alum- or BcfA-adjuvanted vaccines protects from SARS-CoV-2 MA10-induced disease and reduces viral infection of the nose and lungs. **(A)** Prime-pull immunization strategy to elicit mucosal immune response in C57BL/6 or IL-17 KO mice. At 2 wk postboost, mice ($n = 10$ /group) were challenged with the mouse-adapted SARS-CoV-2 strain (MA10). The percent of original body weight on each day postchallenge was calculated through days 9–10 postinfection ($n = 5$ mice/group). **(B)** Weight loss in naive and immunized-challenged C57BL/6 mice. Two-way ANOVA with a Tukey's multiple comparisons test was used to detect differences between all experimental groups. **(C and D)** Viral titer expressed as log median tissue culture infectious dose (TCID₅₀) was quantified from nose (C) and lung (D) of C57BL/6 mice on day 2 postinfection ($n = 5$ mice/group). One-way ANOVA with a Tukey's multiple comparisons test was used to detect differences between experimental groups. **(E)** Weight loss in naive and S/A/B_S/B-immunized IL-17 KO mice challenged with MA10 virus. **(F and G)** Viral titer in nose (F) and lungs (G) of IL-17 KO mice on day 2 postinfection ($n = 4$ –5 mice/group). Significance was calculated by a Student t test. ** $p < 0.01$, **** $p < 0.0001$.

was sacrificed at 2 d postchallenge for lung histological evaluation and quantification of viral PFU in the nose.

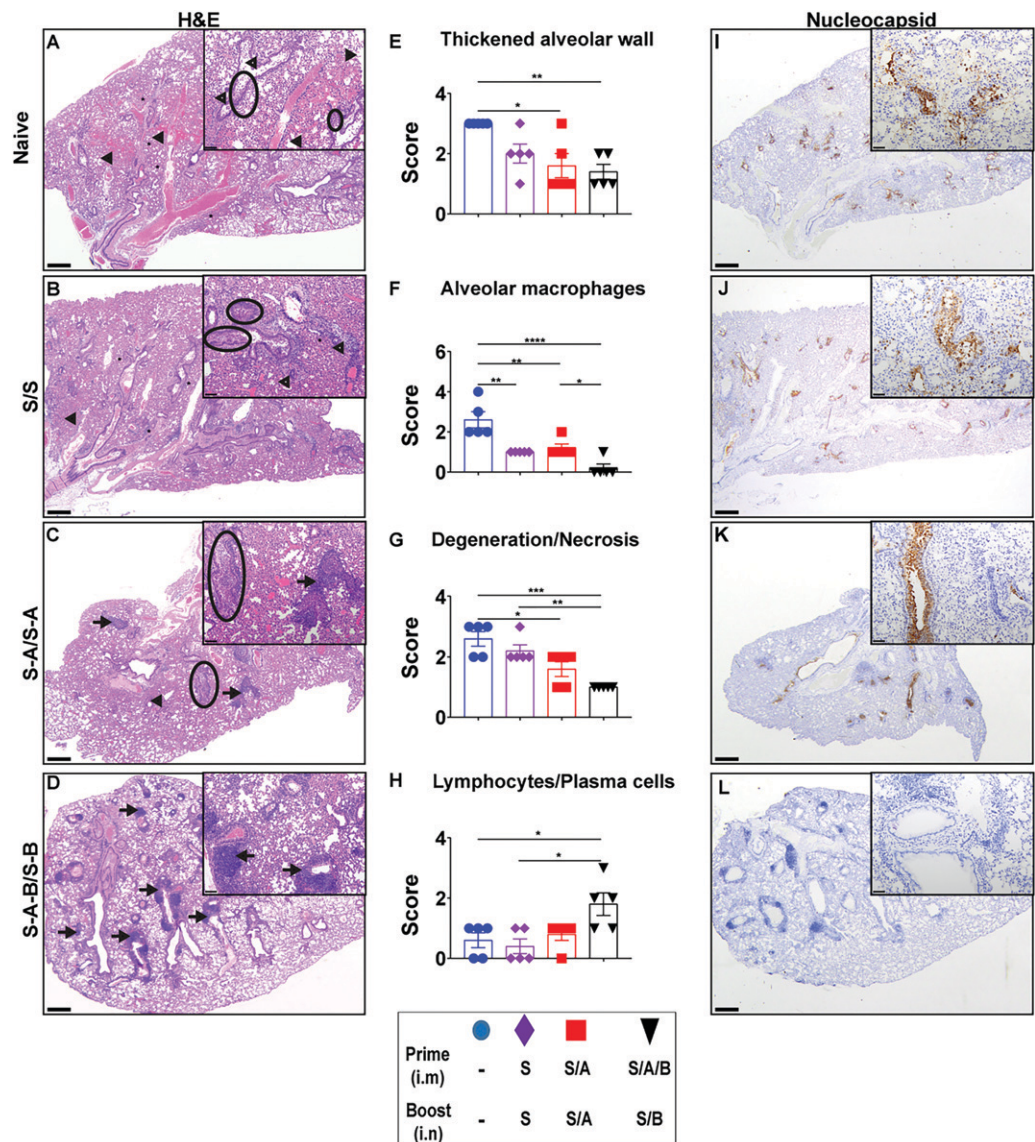
Compared to naive challenged mice, viral load in the nose was significantly reduced in mice immunized with S/A/B_S/B (Fig. 9A) whereas viral load in the noses of mice immunized with SA/SA was not reduced compared with naive challenged or S/A/B_S/B-immunized mice. Thus, mice immunized with the BcfA-adjuvanted vaccine are protected against infection longer than mice immunized with S/A_S/A. Histological evaluation of the lungs (Supplemental Table I) showed type II pneumonitis (Fig. 9B) that was milder in S/A_S/A-immunized mice (Fig. 9C) and absent in S/A/B_S/B-immunized mice (Fig. 9D). Thickening of the alveolar wall (Fig. 9E) and presence of alveolar macrophages (Fig. 9F) was reduced compared with S/A_S/A-immunized mice, suggesting milder disease in this group. Degeneration and necrosis were lower but not significantly reduced (Fig. 9G) whereas lymphocytes and plasma cells were lower than in S/A_S/A-immunized mice (Fig. 9H). Nucleoprotein staining was detected in naive challenged mouse lungs (Fig. 9I) and lungs of S/A_S/A-immunized

mice (Fig. 9J), while nucleoprotein staining was absent from the lungs of S/A/B_S/B-immunized mice (Fig. 9K, Supplemental Table I). Thus, S/A/B_S/B immunization provided longer-lasting protection with milder pathology than S/A_S/A immunization. Weight loss was not observed in naive or immunized mice and was likely due to less efficient infection of 6-mo-old mice.

IL-17⁺ T_{RM}s generated by the BcfA-adjuvanted booster are maintained until 3 mo postboost

We then evaluated the T_{RM} responses in mice immunized with both vaccines. Mice challenged with MA10 virus were harvested at 2 wk postchallenge. The lungs were dissociated and stimulated with the S-specific peptide pool and then stained as described in Fig. 3. Compared to naive challenged mice, the percentages of CD45⁺CD3⁺CD4⁺CD44⁺CD62L⁺CD69⁺ cells were higher in mice immunized with S/A/B_S/B, but not in mice immunized with S/A_S/A (Fig. 10A). The percentage of IFN- γ ⁺ cells was unchanged (Fig. 10B), whereas the percentage of IL-17⁺ cells was increased compared with naive

FIGURE 7. Mice immunized with alum- and BcfA-adjuvanted vaccines have reduced lung pathology and viral Ag compared with alum-adjuvanted vaccines after challenge with SARS-CoV-2 MA10. **(A–D)** Formalin-fixed, paraffin-embedded lungs harvested on day 2 postinfection were sectioned and stained with H&E to evaluate inflammation and tissue damage. **(E–H)** Semiquantitative scoring of alveolar wall thickness (E), presence of alveolar macrophages (F), degeneration and necrosis (G), and presence of lymphocytes and plasma cells (H). **(I–L)** Nucleocapsid viral Ag was evaluated by IHC. H&E staining: original magnification, $\times 2$ (scale bars, 500 μm) with $\times 10$ inset (scale bars, 100 μm). Nucleocapsid staining: original magnification, $\times 2$ with $\times 20$ inset (scale bars, 50 μm). Significance was calculated by ANOVA with a Tukey's multiple comparisons test. * $p < 0.05$, ** $p < 0.01$.



challenged and S/A_S/A-immunized and challenged mice (Fig. 10C). These cell populations were not significantly increased in mice that were immunized but not challenged at 3 mo postboost (data not shown). Thus, sustained protection is accompanied by expansion of $\text{CD4}^+\text{IL-17}^+$ T_{RM} s postinfection in mice immunized with the S/A/B_S/B vaccine combination. An increase in CD8^+ T_{RM} s was not observed at 3 mo postboost, with or without virus challenge (data not shown).

Serum neutralizing Abs are sustained at 3 mo postbooster immunization

Lung (Fig. 10E) and serum (Fig. 10F) IgG and lung (Fig. 10G) and serum (Fig. 10H) IgA remained high in S/A_S/A- and S/A/B_S/B-immunized mice at 3 mo postboost. We tested the ability of serum Abs to neutralize a pseudotyped lentivirus bearing S protein of the SARS-CoV-2 WA1 strain. Mice immunized with alum or BcfA-containing vaccines had high neutralizing activity (Fig. 10 I) compared with naive mice at 2 wk and 3 mo postboost. Serum Abs from both immunized groups neutralized the BA.4/BA.5 (Omicron) recent variant of concern in 40% of the animals at 2 wk and 3 mo postboost (Fig. 10J). Overall, the BcfA-containing vaccine provided longer-lasting protection than the vaccine containing alum alone.

Discussion

Generation of systemic immunity is important for preventing viral infection and dissemination whereas generation of mucosal immunity is critical for sterilizing immunity via clearance of pathogens and infected cells from the respiratory tract (44, 45). Importantly, the ability to reduce viral burden in the nose may be critical for preventing viral transmission (46). Systemic immunization is the approved route for most vaccines, including those against SARS-CoV-2, and it generates strong serum Abs and circulating T cell responses. However, subunit vaccines delivered systemically do not generate mucosal immunity. Immunization i.n. generates T_{RM} responses that provide long-lived protection in the upper respiratory tract (47, 48). We reasoned that i.m. priming and an i.n. booster would elicit strong systemic and mucosal responses and may be especially useful for booster vaccination of individuals already immunized by approved COVID-19 vaccines (45, 49, 50). A similar strategy was tested in macaques that were primed i.m. with S+alum and boosted i.n. with a nanoparticle formulation containing S and CpG, polyinosinic-polycytidylic acid, and IL-15 as adjuvants (34). This regimen reduced viral load in the upper and lower respiratory tract, and it also supports the possibility that the combination of systemic and mucosal immunization will be the most effective in preventing COVID-19 infection.

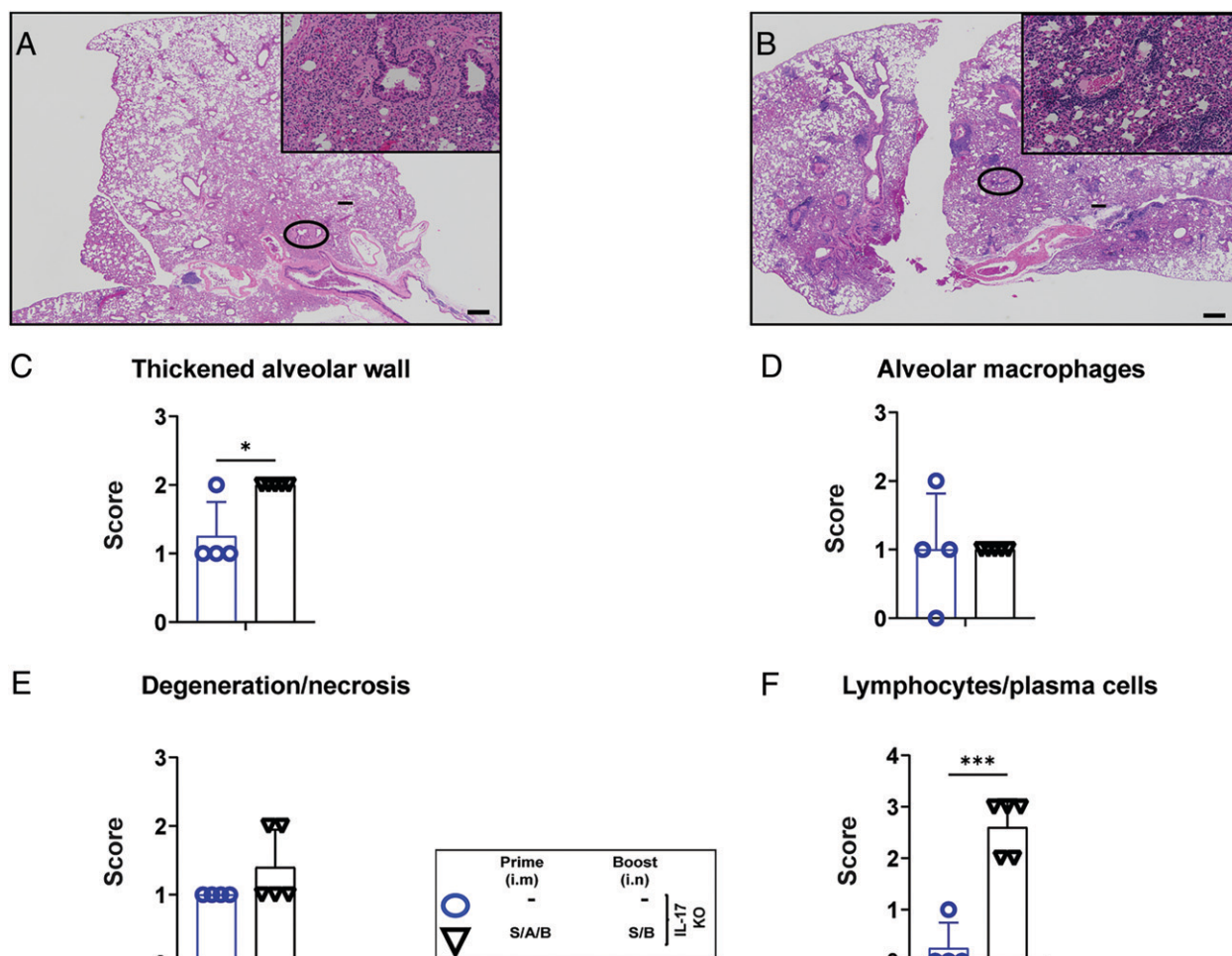


FIGURE 8. IL-17 KO mice immunized with S/A/B_S/B display lung pathology after challenge with SARS-CoV-2 MA10. Formalin-fixed, paraffin-embedded lungs harvested on day 3 postinfection were sectioned and stained with H&E to evaluate inflammation and tissue damage. **(A)** Unimmunized IL-17 KO mice. **(B)** S/A/B_S/B immunized mice. **(C–F)** Semiquantitative scoring of alveolar wall thickness (C), presence of alveolar macrophages (D), degeneration and necrosis (E), and presence of lymphocytes and plasma cells (F) are shown ($n = 4–5$ samples/group). * $p < 0.05$, *** $p < 0.001$, as determined by a Student t test. Blue circles represent naive IL-17 KO mice challenged with MA10. Inverted open triangles indicate S/A/B_S/B-immunized IL-17 KO mice challenged with MA10. Scale bar, 100 μm .

In this study, we report that systemic priming followed by a mucosal booster with a BcfA-containing vaccine generates circulating and tissue-resident T cell and neutralizing Ab responses. This immunization regimen reduces viral titers in the upper and lower respiratory tract. Although the vaccines containing alum alone or alum and BcfA were equally effective in the short term at preventing weight loss and reducing viral load, the BcfA-containing vaccine reduced viral load in the respiratory tract at 3 mo postbooster immunization, suggesting that this formulation and delivery regimen have the potential to reduce transmission of SARS-CoV-2.

The S protein is a target during natural SARS-CoV-2 infection, eliciting S-specific Abs and T cells (30, 40, 51–55). We used a highly stabilized form of the prefusion S protein as the Ag because it is produced more efficiently than the native S and it maintains its structure better than the original 2Pro stabilized form. As such, it elicits neutralizing Abs with greater potency and broader specificity than does postfusion S and is the preferred Ag for next-generation SARS-CoV-2 vaccines (35, 56).

CD8⁺ and CD4⁺ T cell memory responses specific for S as well as for structural proteins M and N are detected in COVID-19 convalescent individuals (17, 30, 57), suggesting that cell-based immunity is critical for protection against SARS-CoV-2. We reported previously that combining BcfA with alum elicited strong Th1/17-polarized

systemic immune responses with attenuation of Th2 responses (26). In this study, our results showed that this heterologous immunization regimen elicited Th1/17 responses in the mucosa. Prime and boost with S/A alone generated CD4⁺IL-5⁺ circulating and T_{RM}S, confirming the Th2 bias of alum-primed immunity. The addition of BcfA to the vaccine elicited IL-17 production from splenocytes with little IL-5, and a booster adjuvanted with BcfA alone generated IL-17-producing T_{RM}S. Both alum and BcfA elicit CD8⁺ T cell responses against other Ags (26). However, we detected minimal CD8⁺ T cell responses to the S protein, suggesting that T cell responses induced by the same adjuvant vary with the antigenic composition of the vaccine. These data further suggest that CD8⁺ T cells are not required for clearance of SARS-CoV-2 from the murine respiratory tract.

Postmortem studies suggest that COVID-19 infection blunts Tfh responses (58) that are critical for induction of sustained humoral immunity. Prime-pull immunization with either alum or alum/BcfA-adjuvanted vaccines generated Tfh cells. This result was also reported by another group where mice immunized i.m. only with an alum-adjuvanted COVID-19 vaccine also generated GC B cells (13). Th1 polarization of Abs elicited by BcfA-adjuvanted vaccines implicates Th1-polarized Tfh cells in this response. Ongoing studies in our group are dissecting Tfh cell phenotypes elicited by these two adjuvants.

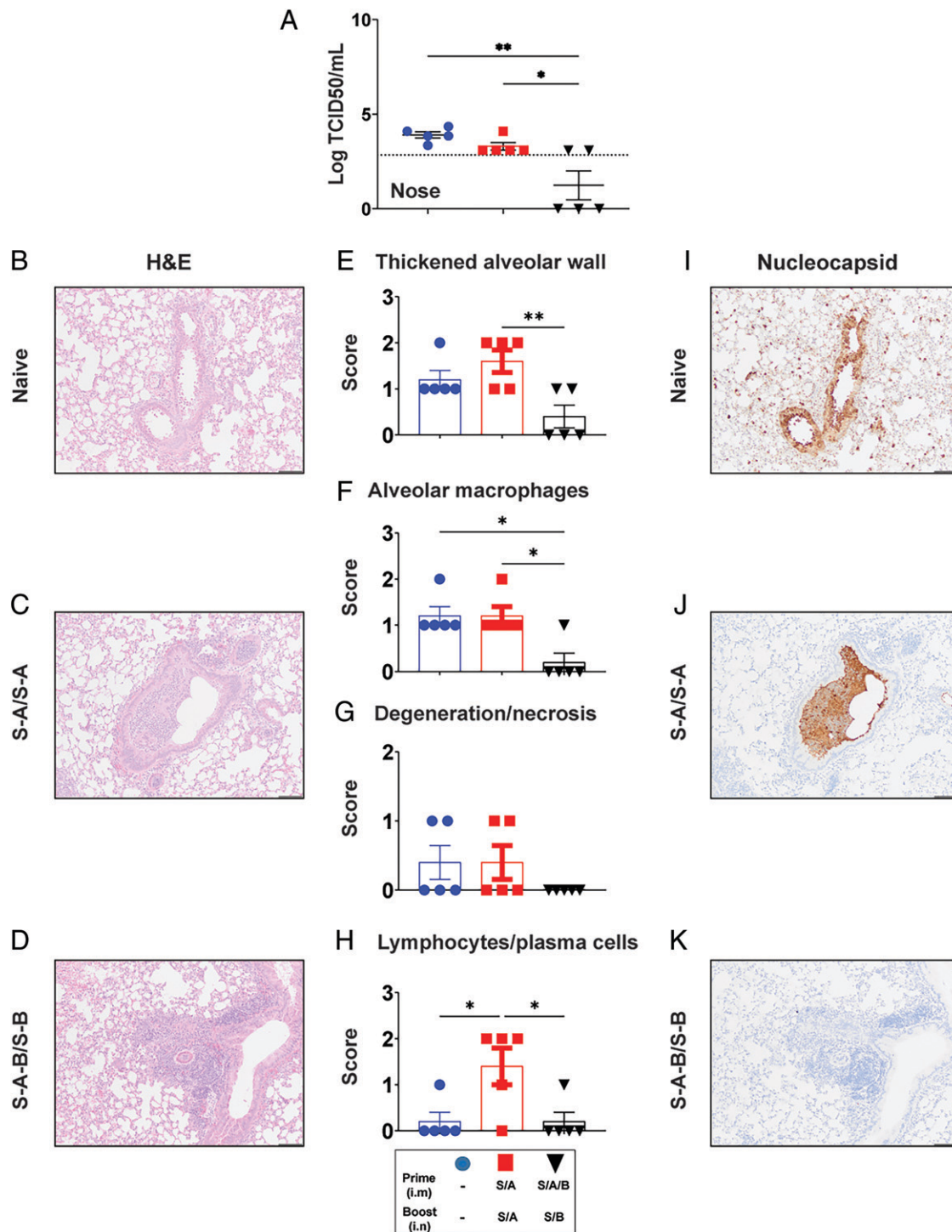


FIGURE 9. Viral titer in the nose and lung pathology is reduced in the nose of S/A/B_S/B-immunized mice challenged at 3 mo postbooster. **(A)** Viral titer expressed as log median tissue culture infectious dose (TCID₅₀) was quantified in the noses of naive or immunized mice challenged with MA10 virus at 3 mo postbooster immunization. Formalin-fixed, paraffin-embedded lung sections were H&E stained and evaluated as in Fig. 7. **(B–D)** Naive (B), S/A_S/A-immunized (C), and S/A/B_S/B-immunized (D) mice. **(E–H)** Semiquantitative scoring of alveolar wall thickness (E), presence of alveolar macrophages (F), degeneration and necrosis (G), and presence of lymphocytes and plasma cells (H). **(I–K)** Nucleocapsid viral Ag was evaluated by IHC. H&E and IHC: original magnification, $\times 10$ (scale bars, 100 μ m). Significance was calculated by ANOVA with a Tukey's multiple comparisons test. * $p < 0.05$, ** $p < 0.01$.

Notably, in contrast to alum-adjuvanted vaccines delivered i.m. only (13, 56), prime-pull immunization with S/A produced IgA in the serum and lungs. Although it is unlikely that alum will be used as an adjuvant for intranasal vaccines, these experiments show that changing the delivery route of the vaccine alters the composition of the immune response. Although alum- and alum/BcfA-adjuvanted vaccines induced mucosal IgA and IgG, the IgG avidity and ratio of

IgG2/IgG1 was higher in the lungs of mice primed with S/A/B and boosted with S/B. In contrast, serum Abs in both vaccine groups were similar in avidity and IgG2/IgG1 ratio, suggesting that the mucosal booster with S/B resulted in Ab maturation in situ.

Weight loss is often a manifestation of disease in young or elderly mice challenged with SARS-CoV-2 (10, 13). Whereas naive mice challenged with MA10 initially lost weight, mice immunized with

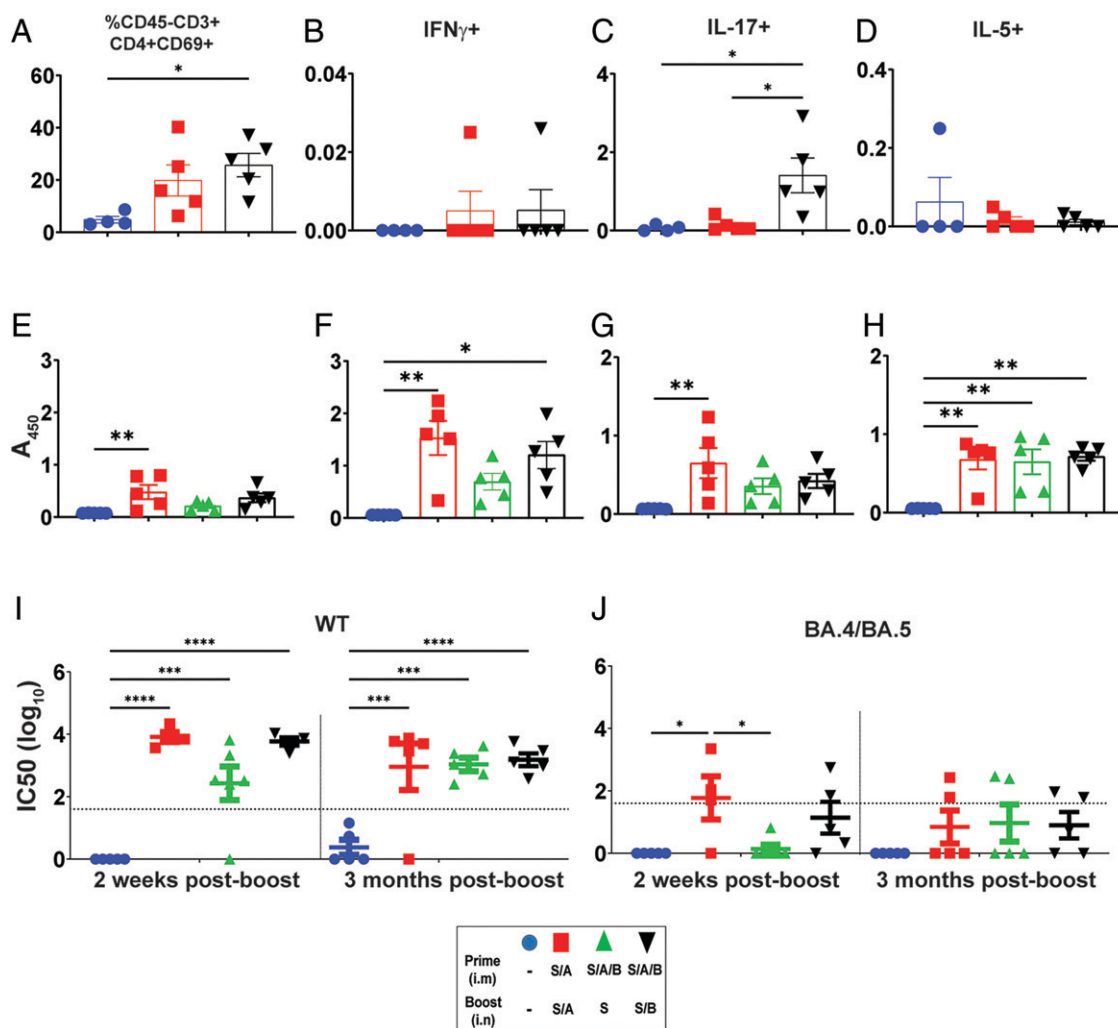


FIGURE 10. T_{RMS} and systemic humoral responses are sustained at 3 mo postbooster immunization. Lung cells were stimulated for 6 h with S-derived peptide pools (S1 and S2) at a concentration of 1 μ g/ml in the presence of protein transport inhibitors. Surface staining and ICS was conducted to analyze $CD45^{+}$ resident T cells. (A) Percentage of $CD45^{+}CD3^{+}CD4^{+}CD44^{-}CD62L^{-}CD69^{+}$ Ag-experienced $CD4^{+}$ T_{RMS} . (B–D) Percentage of $IFN-\gamma^{+}$ (B), $IL-17^{+}$ (C), and $IL-5^{+}$ (D) cells. ELISA analysis evaluated S-specific Abs in lung homogenates and serum. (E–H) Lung IgA (E), serum IgA (F), lung IgG (G), serum IgG (H). A glucose-based lentiviral SARS-CoV-2 pseudovirus expressing the wild-type (WT) S protein or the BA.4/BA.5 (Omicron) variant was used to determine the neutralizing activity of serum Abs. (I and J) For the WT S protein (I) and the BA.4/BA.5 (Omicron) variant (J), results from 2 wk and 3 mo postboost are shown. Differences between experimental groups were determined by a one-way ANOVA with a Tukey's multiple comparisons test. * $p < 0.05$, ** $p < 0.01$, *** $p < 0.001$, **** $p < 0.0001$. $n = 5$ animals per group; mean and SEM of the results are displayed.

either S/A_S/A or S/A_B_S/B did not lose a significant amount of weight after challenge. Mice immunized with alum- or alum/BcfA-containing vaccines had low viral titer in the nose and lungs, suggesting that both formulations provide similar protection against severe disease. We tested the importance of the $IL-17^{+}$ T cells elicited by S/A_B_S/B immunization in protection against disease and respiratory pathology. In $IL-17$ KO mice immunized with S/A_B_S/B, viral load in the nose did not decline and only declined slightly in the lungs, suggesting that $IL-17$ generated by vaccination with the BcfA-adjuvanted formulation is important for the antiviral response. In subsequent work we will test the relative importance of different $IL-17$ -producing immune cell subsets to protection.

Sustained immune responses that prevent disease and infection are key components of effective vaccines. Systemic and mucosal Abs were detected at 3 mo postbooster with the alum- and alum/BcfA-containing vaccines and maintained neutralizing activity against the pseudotyped virus expressing an early isolate S protein. Interestingly, although not statistically significant, serum from 40% of the immunized animals also neutralized the BA.4/5 Omicron variant virus

at 3 mo postboost. Humans immunized with two doses of mRNA vaccines encoding S protein from early SARS-CoV-2 isolates do not neutralize the Omicron variants (59, 60). Following virus challenge at 3 mo postboost, $IL-17^{+}$ T_{RMS} expanded in the lungs of mice immunized with the BcfA-containing vaccine. Notably, viral titer was reduced in the noses of these immunized mice but was not reduced in mice immunized with the alum-adjuvanted vaccine. Histopathology and IHC analysis also revealed an important distinction between the vaccine formulations. S/A-immunized mice had evidence of pneumonitis and epithelial damage and expression of nucleoprotein Ag when challenged at 2 wk and 3 mo postbooster. In contrast, the lungs of mice immunized with BcfA-adjuvanted vaccines had a leukocyte infiltrate, little evidence of damage to the lung tissue, and complete absence of nucleoprotein expression at both time points. Overall, these data suggest that protection against SARS-CoV-2 infection is sustained with the addition of BcfA to the vaccine.

Multiple studies suggested a significant role for $IL-17$ in SARS-CoV-2 infection-induced immunopathology (61–63) and argued for targeting $IL-17$ as a plausible therapeutic strategy (62, 64–66). In

addition, some studies proposed Th17-polarized responses to be the key player in VAERD instead of Th2, although current evidence is inconclusive (15, 67). Our results suggest that activation of Th17 responses while attenuating Th2 responses limits pathology and protects against COVID-19 infection. Testing of BcfA-adjuvanted vaccines in larger animal models to validate these results in mice will be necessary prior to clinical trials.

Taken together, our data show that prime-pull immunization with a combination of alum and BcfA as adjuvants generates S-specific systemic and mucosal Th1/17-polarized immune responses that are highly effective at preventing SARS-CoV-2 infection and preventing respiratory damage. Given that global vaccination rates are on the rise, there will be an increasing need for booster vaccines that extend protection provided by currently approved mRNA vaccines. Thus, it will be important to test whether an i.n. booster with S/B generates mucosal immunity in individuals previously immunized with mRNA vaccines, and thereby increases the longevity of protection.

Acknowledgments

We thank Jason McLellan for the plasmid expressing the HexaPro stabilized version of the S protein. We acknowledge the BSL-3 program at The Ohio State University.

Disclosures

The authors have no financial conflicts of interest.

References

- Wang, C., P. W. Horby, F. G. Hayden, and G. F. Gao. 2020. A novel coronavirus outbreak of global health concern. *Lancet* 395: 470–473.
- Wu, F., S. Zhao, B. Yu, Y.-M. Chen, W. Wang, Z.-G. Song, Y. Hu, Z.-W. Tao, J.-H. Tian, Y.-Y. Pei, et al. 2020. A new coronavirus associated with human respiratory disease in China. [Published erratum appears in 2020 *Nature* 580: E7.] *Nature* 579: 265–269.
- Zhu, N., D. Zhang, W. Wang, X. Li, B. Yang, J. Song, X. Zhao, B. Huang, W. Shi, R. Lu, et al.; China Novel Coronavirus Investigating and Research Team. 2020. A novel coronavirus from patients with pneumonia in China, 2019. *N. Engl. J. Med.* 382: 727–733.
- Lederer, K., D. Castaño, D. Gómez Atria, T. H. Oguin III, S. Wang, T. B. Manzoni, H. Muramatsu, M. J. Hogan, F. Amanat, P. Cherubin, et al. 2020. SARS-CoV-2 mRNA vaccines foster potent antigen-specific germinal center responses associated with neutralizing antibody generation. *Immunity* 53: 1281–1295.e5.
- Patel, K. P., S. R. Vunnam, P. A. Patel, K. L. Krill, P. M. Korbitz, J. P. Gallagher, J. E. Suh, and R. R. Vunnam. 2020. Transmission of SARS-CoV-2: an update of current literature. *Eur. J. Clin. Microbiol. Infect. Dis.* 39: 2005–2011.
- Lippi, G., F. Sanchis-Gomar, and B. M. Henry. 2020. COVID-19: unravelling the clinical progression of nature's virtually perfect biological weapon. *Ann. Transl. Med.* 8: 693.
- Bai, Y., L. Yao, T. Wei, F. Tian, D. Y. Jin, L. Chen, and M. Wang. 2020. Presumed asymptomatic carrier transmission of COVID-19. *JAMA* 323: 1406–1407.
- Gandhi, M., D. S. Yokoe, and D. V. Havlir. 2020. Asymptomatic transmission, the Achilles' heel of current strategies to control Covid-19. *N. Engl. J. Med.* 382: 2158–2160.
- Case, J. B., E. S. Winkler, J. M. Errico, and M. S. Diamond. 2021. On the road to ending the COVID-19 pandemic: are we there yet? *Virology* 557: 70–85.
- Tostanoski, L. H., L. E. Gralinski, D. R. Martinez, A. Schaefer, S. H. Mahrokhian, Z. Li, F. Nampanya, H. Wan, J. Yu, A. Chang, et al. 2021. Protective efficacy of rhesus adenovirus COVID-19 vaccines against mouse-adapted SARS-CoV-2. *J. Virol.* 95: e0097421.
- Ketas, T. J., D. Chaturbhuj, V. M. C. Portillo, E. Francomano, E. Golden, S. Chandrasekhar, G. Debnath, R. Díaz-Tapia, A. Yasmeen, K. D. Kramer, et al. 2021. Antibody responses to SARS-CoV-2 mRNA vaccines are detectable in saliva. *Pathog. Immun.* 6: 116–134.
- Mades, A., P. Chellamathu, L. Lopez, N. Kojima, M. A. MacMullan, N. Denny, A. N. Angel, J. G. Casian, M. Brobeck, N. Nirema, et al. 2021. Detection of persistent SARS-CoV-2 IgG antibodies in oral mucosal fluid and upper respiratory tract specimens following COVID-19 mRNA vaccination. *Sci. Rep.* 11: 24448.
- DiPiazza, A. T., S. R. Leist, O. M. Abiona, J. I. Molina, A. Werner, M. Mina, B. M. Nagata, K. W. Bock, E. Phung, A. Schaefer, et al. 2021. COVID-19 vaccine mRNA-1273 elicits a protective immune profile in mice that is not associated with vaccine-enhanced disease upon SARS-CoV-2 challenge. *Immunity* 54: 1869–1882.e6.
- Halstead, S. B., and L. Katzelnick. 2020. COVID-19 vaccines: should we fear ADE? *J. Infect. Dis.* 222: 1946–1950.
- Liang, Z., H. Zhu, X. Wang, B. Jing, Z. Li, X. Xia, H. Sun, Y. Yang, W. Zhang, L. Shi, et al. 2020. Adjuvants for coronavirus vaccines. *Front. Immunol.* 11: 589833.
- Seephetdee, C., N. Buasri, K. Bhukhai, K. Srisanga, S. Manopwisedjaroen, S. Lertjintanakit, N. Phueakphud, C. Pakirany, N. Kangwanrangsan, S. Srichatrapimuk, et al. 2021. Mice immunized with the vaccine candidate HexaPro spike produce neutralizing antibodies against SARS-CoV-2. *Vaccines (Basel)* 9: 498.
- Sekine, T., A. Perez-Potti, O. Rivera-Ballesteros, K. Strålin, J. B. Gorin, A. Olsson, S. Llewellyn-Lacey, H. Kamal, G. Bogdanovic, S. Muschiol, et al.; Karolinska COVID-19 Study Group. 2020. Robust T cell immunity in convalescent individuals with asymptomatic or mild COVID-19. *Cell* 183: 158–168.e14.
- Graham, B. S., G. S. Henderson, Y. W. Tang, X. Lu, K. M. Neuzil, and D. G. Colley. 1993. Priming immunization determines T helper cytokine mRNA expression patterns in lungs of mice challenged with respiratory syncytial virus. *J. Immunol.* 151: 2032–2040.
- Kim, H. W., J. G. Canchola, C. D. Brandt, G. Pyles, R. M. Chanock, K. Jensen, and R. H. Parrott. 1969. Respiratory syncytial virus disease in infants despite prior administration of antigenic inactivated vaccine. *Am. J. Epidemiol.* 89: 422–434.
- Fulginiti, V. A., J. J. Eller, A. W. Downie, and C. H. Kempe. 1967. Altered reactivity to measles virus. Atypical measles in children previously immunized with inactivated measles virus vaccines. *JAMA* 202: 1075–1080.
- Nader, P. R., M. S. Horwitz, and J. Rousseau. 1968. Atypical exanthem following exposure to natural measles: eleven cases in children previously inoculated with killed vaccine. *J. Pediatr.* 72: 22–28.
- Agrawal, A. S., X. Tao, A. Algaissi, T. Garron, K. Narayanan, B. H. Peng, R. B. Couch, and C. T. K. Tseng. 2016. Immunization with inactivated Middle East respiratory syndrome coronavirus vaccine leads to lung immunopathology on challenge with live virus. *Hum. Vaccin. Immunother.* 12: 2351–2356.
- Czub, M., H. Weingartl, S. Czub, R. He, and J. Cao. 2005. Evaluation of modified vaccinia virus Ankara based recombinant SARS vaccine in ferrets. *Vaccine* 23: 2273–2279.
- See, R. H., A. N. Zakhartchouk, M. Petric, D. J. Lawrence, C. P. Y. Mok, R. J. Hogan, T. Rowe, L. A. Zitzow, K. P. Karunakaran, M. M. Hitt, et al. 2006. Comparative evaluation of two severe acute respiratory syndrome (SARS) vaccine candidates in mice challenged with SARS coronavirus. *J. Gen. Virol.* 87: 641–650.
- Tseng, C. T., E. Sbrana, N. Iwata-Yoshikawa, P. C. Newman, T. Garron, R. L. Atmar, C. J. Peters, and R. B. Couch. 2012. Immunization with SARS coronavirus vaccines leads to pulmonary immunopathology on challenge with the SARS virus. [Published erratum appears in 2012 *PLoS One* 7: doi:10.1371/annotation/2965cfac-b77d-4014-8b7b-236e01a35492.] *PLoS One* 7: e35421.
- Jennings-Gee, J., S. Quataert, T. Ganguly, R. D'Agostino, Jr., R. Deora, and P. Dubey. 2018. The adjuvant Bordetella colonization factor A attenuates alum-induced Th2 responses and enhances Bordetella pertussis clearance from mouse lungs. *Infect. Immun.* 86: e00935-17.
- Sukumar, N., C. F. Love, M. S. Conover, N. D. Kock, P. Dubey, and R. Deora. 2009. Active and passive immunizations with *Bordetella* colonization factor A protect mice against respiratory challenge with *Bordetella bronchiseptica*. *Infect. Immun.* 77: 885–895.
- Bolles, M., D. Deming, K. Long, S. Agnihotram, A. Whitmore, M. Ferris, W. Funkhouser, L. Gralinski, A. Tatura, M. Heise, and R. S. Baric. 2011. A double-inactivated severe acute respiratory syndrome coronavirus vaccine provides incomplete protection in mice and induces increased eosinophilic proinflammatory pulmonary response upon challenge. *J. Virol.* 85: 12201–12215.
- Honda-Okubo, Y., D. Barnard, C. H. Ong, B.-H. Peng, C.-T. K. Tseng, and N. Petrovsky. 2015. Severe acute respiratory syndrome-associated coronavirus vaccines formulated with delta inulin adjuvants provide enhanced protection while ameliorating lung eosinophilic immunopathology. *J. Virol.* 89: 2995–3007.
- Grifoni, A., D. Weiskopf, S. I. Ramirez, J. Mateus, J. M. Dan, C. R. Moderbacher, S. A. Rawlings, A. Sutherland, L. Premkumar, R. S. Jodi, et al. 2020. Targets of T cell responses to SARS-CoV-2 coronavirus in humans with COVID-19 disease and unexposed individuals. *Cell* 181: 1489–1501.e15.
- McPherson, C., R. Chubet, K. Holtz, Y. Honda-Okubo, D. Barnard, M. Cox, and N. Petrovsky. 2016. Development of a SARS coronavirus vaccine from recombinant spike protein plus delta inulin adjuvant. *Methods Mol. Biol.* 1403: 269–284.
- Yasui, F., C. Kai, M. Kitabatake, S. Inoue, M. Yoneda, S. Yokochi, R. Kase, S. Sekiguchi, K. Morita, T. Hishima, et al. 2008. Prior immunization with severe acute respiratory syndrome (SARS)-associated coronavirus (SARS-CoV) nucleocapsid protein causes severe pneumonia in mice infected with SARS-CoV. *J. Immunol.* 181: 6337–6348.
- Roces, C. B., M. T. Hussain, S. T. Schmidt, D. Christensen, and Y. Perrie. 2019. Investigating prime-pull vaccination through a combination of parenteral vaccination and intranasal boosting. *Vaccines (Basel)* 8: 10.
- Sui, Y., J. Li, R. Zhang, S. K. Prabhu, H. Andersen, D. Venzon, A. Cook, R. Brown, E. Teow, J. Velasco, et al. 2021. Protection against SARS-CoV-2 infection by a mucosal vaccine in rhesus macaques. *JCI Insight* 6: e148494.
- Hsieh, C. L., J. A. Goldsmith, J. M. Schaub, A. M. DiVenere, H. C. Kuo, K. Javanmardi, K. C. Le, D. Wrapp, A. G. Lee, Y. Liu, et al. 2020. Structure-based design of prefusion-stabilized SARS-CoV-2 spikes. *Science* 369: 1501–1505.
- Leist, S. R., K. H. Dinno III, A. Schäfer, L. V. Tse, K. Okuda, Y. J. Hou, A. West, C. E. Edwards, W. Sanders, E. J. Fritch, et al. 2020. A mouse-adapted SARS-CoV-2 induces acute lung injury and mortality in standard laboratory mice. *Cell* 183: 1070–1085.e12.
- Anderson, K. G., K. Mayer-Barber, H. Sung, L. Beura, B. R. James, J. J. Taylor, L. Qunaj, T. S. Griffith, V. Vezys, D. L. Barber, and D. Masopust. 2014. Intravascular staining for discrimination of vascular and tissue leukocytes. *Nat. Protoc.* 9: 209–222.
- Wilks, M. M., A. Misiak, R. M. McManus, A. C. Allen, M. A. Lynch, and K. H. G. Mills. 2017. Lung CD4 tissue-resident memory T cells mediate adaptive immunity induced by previous infection of mice with *Bordetella pertussis*. *J. Immunol.* 199: 233–243.

39. Macdonald, R. A., C. S. Hosking, and C. L. Jones. 1988. The measurement of relative antibody affinity by ELISA using thiocyanate elution. *J. Immunol. Methods* 106: 191–194.
40. Zeng, C., J. P. Evans, R. Pearson, P. Qu, Y. M. Zheng, R. T. Robinson, L. Hall-Stoodley, J. Yount, S. Pannu, R. K. Mallampalli, et al. 2020. Neutralizing antibody against SARS-CoV-2 spike in COVID-19 patients, health care workers, and convalescent plasma donors. *JCI Insight* 5: e143213.
41. Crotty, S. 2014. T follicular helper cell differentiation, function, and roles in disease. *Immunity* 41: 529–542.
42. Cyster, J. G., and C. D. C. Allen. 2019. B cell responses: cell interaction dynamics and decisions. *Cell* 177: 524–540.
43. Kräutler, N. J., D. Suan, D. Butt, K. Bourne, J. R. Hermes, T. D. Chan, C. Sundling, W. Kaplan, P. Schofield, J. Jackson, et al. 2017. Differentiation of germinal center B cells into plasma cells is initiated by high-affinity antigen and completed by Tfh cells. *J. Exp. Med.* 214: 1259–1267.
44. Matuchansky, C. 2021. Mucosal immunity to SARS-CoV-2: a clinically relevant key to deciphering natural and vaccine-induced defences. *Clin. Microbiol. Infect.* 27: 1724–1726.
45. Russell, M. W., Z. Moldoveanu, P. L. Ogra, and J. Mestecky. 2020. Mucosal immunity in COVID-19: a neglected but critical aspect of SARS-CoV-2 infection. *Front. Immunol.* 11: 611337.
46. Gallo, O., L. G. Locatello, A. Mazzoni, L. Novelli, and F. Annunziato. 2021. The central role of the nasal microenvironment in the transmission, modulation, and clinical progression of SARS-CoV-2 infection. *Mucosal Immunol.* 14: 305–316.
47. Allen, A. C., M. M. Wilk, A. Misiak, L. Borkner, D. Murphy, and K. H. G. Mills. 2018. Sustained protective immunity against *Bordetella pertussis* nasal colonization by intranasal immunization with a vaccine-adjuvant combination that induces IL-17-secreting T_{RM} cells. *Mucosal Immunol.* 11: 1763–1776.
48. Wilk, M. M., and K. H. G. Mills. 2018. CD4 T_{RM} cells following infection and immunization: implications for more effective vaccine design. *Front. Immunol.* 9: 1860.
49. Lavelle, E. C., and R. W. Ward. 2022. Mucosal vaccines—fortifying the frontiers. *Nat. Rev. Immunol.* 22: 236–250.
50. Lycke, N. 2012. Recent progress in mucosal vaccine development: potential and limitations. *Nat. Rev. Immunol.* 12: 592–605.
51. Hellerstein, M. 2020. What are the roles of antibodies versus a durable, high quality T-cell response in protective immunity against SARS-CoV-2? *Vaccine X* 6: 100076.
52. Le Bert, N., A. T. Tan, K. Kunasegaran, C. Y. L. Tham, M. Hafezi, A. Chia, M. H. Y. Chng, M. Lin, N. Tan, M. Linster, et al. 2020. SARS-CoV-2-specific T cell immunity in cases of COVID-19 and SARS, and uninfected controls. *Nature* 584: 457–462.
53. Peng, Y., A. J. Mentzer, G. Liu, X. Yao, Z. Yin, D. Dong, W. Dejnirattisai, T. Rostron, P. Supasa, C. Liu, et al.; ISARIC4C Investigators. 2020. Broad and strong memory CD4⁺ and CD8⁺ T cells induced by SARS-CoV-2 in UK convalescent individuals following COVID-19. *Nat. Immunol.* 21: 1336–1345.
54. Tan, Y., F. Liu, X. Xu, Y. Ling, W. Huang, Z. Zhu, M. Guo, Y. Lin, Z. Fu, D. Liang, et al. 2020. Durability of neutralizing antibodies and T-cell response post SARS-CoV-2 infection. *Front. Med.* 14: 746–751.
55. Wajnberg, A., F. Amanat, A. Firpo, D. R. Altman, M. J. Bailey, M. Mansour, M. McMahon, P. Meade, D. R. Mendu, K. Muellers, et al. 2020. Robust neutralizing antibodies to SARS-CoV-2 infection persist for months. *Science* 370: 1227–1230.
56. Arunachalam, P. S., A. C. Walls, N. Golden, C. Atyeo, S. Fischinger, C. Li, P. Aye, M. J. Navarro, L. Lai, V. V. Edara, et al. 2021. Adjuvanting a subunit COVID-19 vaccine to induce protective immunity. *Nature* 594: 253–258.
57. Kared, H., A. D. Redd, E. M. Bloch, T. S. Bonny, H. Sumatoh, F. Kairi, D. Carbajo, B. Abel, E. W. Newell, M. P. Bettinotti, et al. 2021. SARS-CoV-2-specific CD8⁺ T cell responses in convalescent COVID-19 individuals. *J. Clin. Invest.* 131: e145476.
58. Kaneko, N., H. H. Kuo, J. Boucay, J. R. Farmer, H. Allard-Chamard, V. S. Mahajan, A. Piechocka-Trocha, K. Lefteri, M. Osborn, J. Bals, et al.; Massachusetts Consortium on Pathogen Readiness Specimen Working Group. 2020. Loss of Bcl-6-expressing T follicular helper cells and germinal centers in COVID-19. *Cell* 183: 143–157.e13.
59. Wang, P., M. S. Nair, L. Liu, S. Iketani, Y. Luo, Y. Guo, M. Wang, J. Yu, B. Zhang, P. D. Kwong, et al. 2021. Antibody resistance of SARS-CoV-2 variants B.1.351 and B.1.1.7. *Nature* 593: 130–135.
60. Wang, Q., Y. Guo, S. Iketani, M. S. Nair, Z. Li, H. Mohri, M. Wang, J. Yu, A. D. Bowen, J. Y. Chang, et al. 2022. Antibody evasion by SARS-CoV-2 Omicron subvariants BA.2.12.1, BA.4 and BA.5. *Nature* 608: 603–608.
61. Parackova, Z., M. Bloomfield, A. Klocperk, and A. Sediva. 2021. Neutrophils mediate Th17 promotion in COVID-19 patients. *J. Leukoc. Biol.* 109: 73–76.
62. Wu, D., and X. O. Yang. 2020. TH17 responses in cytokine storm of COVID-19: an emerging target of JAK2 inhibitor fedratinib. *J. Microbiol. Immunol. Infect.* 53: 368–370.
63. Xu, Z., L. Shi, Y. Wang, J. Zhang, L. Huang, C. Zhang, S. Liu, P. Zhao, H. Liu, L. Zhu, et al. 2020. Pathological findings of COVID-19 associated with acute respiratory distress syndrome. *Lancet Respir. Med.* 8: 420–422.
64. Orlov, M., P. L. Wander, E. D. Morrell, C. Mikacenic, and M. M. Wurfel. 2020. A case for targeting Th17 cells and IL-17A in SARS-CoV-2 infections. *J. Immunol.* 205: 892–898.
65. Pacha, O., M. A. Sallman, and S. E. Evans. 2020. COVID-19: a case for inhibiting IL-17? *Nat. Rev. Immunol.* 20: 345–346.
66. Sarmiento-Monroy, J. C., R. Parra-Medina, E. Garavito, and A. Rojas-Villarraga. 2021. T helper 17 response to severe acute respiratory syndrome coronavirus 2: a type of immune response with possible therapeutic implications. *Viral Immunol.* 34: 190–200.
67. Hotez, P. J., M. E. Bottazzi, and D. B. Corry. 2020. The potential role of Th17 immune responses in coronavirus immunopathology and vaccine-induced immune enhancement. *Microbes Infect.* 22: 165–167.